

# EXPERIMENTAL ASSESSMENT OF AGGREGATE SURFACING MATERIALS

---

FHWA/MT-07-011/8117-30

---

*Final Report*

*prepared for*  
THE STATE OF MONTANA  
DEPARTMENT OF TRANSPORTATION

*in cooperation with*  
THE U.S. DEPARTMENT OF TRANSPORTATION  
FEDERAL HIGHWAY ADMINISTRATION

---

*July 2007*

*prepared by*  
Robert Mokwa  
Nicholas Trimble  
Eli Cuelho

Montana State University - Bozeman



RESEARCH PROGRAMS



You are free to copy, distribute, display, and perform the work; make derivative works; make commercial use of the work under the condition that you give the original author and sponsor credit. For any reuse or distribution, you must make clear to others the license terms of this work. Any of these conditions can be waived if you get permission from the sponsor. Your fair use and other rights are in no way affected by the above.

# **EXPERIMENTAL ASSESSMENT OF AGGREGATE SURFACING MATERIALS**

*Final Project Report*

Prepared by:

**Dr. Robert Mokwa, P.E.**

Associate Professor, Civil Engineering Department

**Nicholas Trimble**

Graduate Student, Western Transportation Institute

**Eli Cuelho, P.E.**

Research Engineer, Western Transportation Institute

of the

College of Engineering  
Montana State University – Bozeman

State of Montana  
Department of Transportation  
Research Programs

in cooperation with the

U.S. Department of Transportation  
Federal Highway Administration

June 2007

## TECHNICAL REPORT DOCUMENTATION PAGE

1. Report No.: FHWA/MT-07-011/8117-30	2. Government Access No.:	3. Recipient's Catalog No.:	
4. Title and Subtitle: Experimental Assessment of Aggregate Surfacing Materials	5. Report Date: June 30, 2007		
	6. Performing Organization Code:		
7. Author(s): Robert Mokwa, Nicholas Trimble, and Eli Cuelho	8. Performing Organization Report Code:		
9. Performing Organization Name and Address: Montana State University Civil Engineering Dept., Bozeman, Montana 59717	10. Work Unit No.:		
	11. Contract or Grant No.: 8117-30		
12. Sponsoring Agency Name and Address: Research Programs Montana Department of Transportation 2701 Prospect Avenue Helena, Montana 59620-1001	13. Type of Report and Period Covered: Final Report January 2006 – June 2007		
	14. Sponsoring Agency Code: 5401		
15. Supplementary Notes: Research performed in cooperation with the Montana Department of Transportation and the U.S. Department of Transportation, Federal Highway Administration. This report can be found at <a href="http://www.mdt.mt.gov/research/docs/research_proj/exp_assess/final_report.pdf">http://www.mdt.mt.gov/research/docs/research_proj/exp_assess/final_report.pdf</a> .			
16. Abstract: <p>An extensive suite of geotechnical laboratory tests were conducted to quantify differences in engineering properties of three crushed aggregates commonly used on Montana highway projects. The material types are identified in the Montana Supplemental Specifications as CBC-6A, CBC-5A, and CTS-2A. Results from R-value tests and direct shear tests performed on large samples (12 in by 12 in) indicates the CBC-6A aggregates generally exhibited the highest strength and stiffness of the three material types. In terms of strength parameters, there was no statistically significant difference between CBC-5A and CTS-2A materials. The CBC-6A and 5A materials exhibited similar average R-values, which were both slightly greater than the CTS-2A materials. Overall, the CTS-2A materials generally exhibited the lowest average strength and stiffness. Although this material was the poorest performer when compared to the two CBC materials, it still exhibited relatively high strength and stiffness. Drainage capacity was quantified by conducting multiple saturated constant head permeability tests on 10-inch-diameter samples of each material type. The CBC-6A and CTS-2A materials had the highest average permeability values, while the CBC-5A materials had the lowest. Permeability was shown to depend more on the fine fraction void ratio (<math>e_f</math>) than on aggregate type or maximum particle size. An analytical method of predicting permeability based on <math>e_f</math> was developed, which will allow MDT designers to estimate permeability based on gradation and state of compaction.</p> <p>Overall, the CBC-6A materials were generally the best performers in this study. In general, the CBC-5A aggregates exhibited the second highest strength and stiffness, but also had the lowest drainage capacity. The CTS-2A aggregates exhibited the lowest strength and stiffness, but had relatively good drainage capacity. The ability to substitute CTS-2A material for CBC aggregates depends on the relative importance that is assigned to strength, stiffness, and drainage in the pavement design model.</p>			
17. Key Words: Crushed Base Course, CBC, Crushed Top Surfacing, CTS, Base Course, Base Course Aggregate, Permeability		18. Distribution Statement: No restrictions. This document is available through National Tech. Info. Service, Springfield, VA 22161.	
19. Security Classif. (of this report): Unclassified	20. Security Classif. (of this page): Unclassified	21. No. of Pages: 74	22. Price:

---

## **DISCLAIMER STATEMENT**

This document is disseminated under the sponsorship of the Montana Department of Transportation and the United States Department of Transportation in the interest of information exchange. The State of Montana and the United States Government assume no liability of its contents or use thereof.

The contents of this report reflect the views of the authors, who are responsible for the facts and accuracy of the data presented herein. The contents do not necessarily reflect the official policies of the Montana Department of Transportation or the United States Department of Transportation.

The State of Montana and the United States Government do not endorse products of manufacturers. Trademarks or manufacturers' names appear herein only because they are considered essential to the object of this document.

This report does not constitute a standard, specification, or regulation.

## **ALTERNATIVE FORMAT STATEMENT**

MDT attempts to provide accommodations for any known disability that may interfere with a person participating in any service, program, or activity of the Department. Alternative accessible formats of this information will be provided upon request. For further information, call (406) 444-7693, TTY (800) 335-7592, or Montana Relay at 711.

## **ACKNOWLEDGEMENTS**

The authors gratefully acknowledge the valuable assistance provided by MDT personnel in obtaining soil samples from around the state. Special thanks and acknowledgement are extended to Mike Mullings for conducting R-value tests on all the samples.

Acknowledgement of financial support for this research is extended to the Montana Department of Transportation and the Research and Innovative Technology Administration (RITA) at the United States Department of Transportation through the Western Transportation Institute at Montana State University.

---

## UNIT CONVERSIONS

Measurement	Metric	English
Length	1 cm	0.394 in
	1 m	3.281 ft
	1 km	0.621 mile
Area	1 cm <sup>2</sup>	0.155 in <sup>2</sup>
	1 m <sup>2</sup>	1.196 yd <sup>2</sup>
Volume	1 m <sup>3</sup>	1.308 yd <sup>3</sup>
	1 ml	0.034 oz
Force	1 N	0.225 lbf
	1 kN	0.225 kip
Stress	1 MPa	145 psi
	1 GPa	145 ksi
Unit Weight	1 kN/m <sup>3</sup>	6.36 lb/ft <sup>3</sup>
Permeability	1 cm/s	118.1 ft/hr

## TABLE OF CONTENTS

Executive Summary .....	ix
1 Introduction.....	1
2 Methods & Materials .....	2
2.1 Laboratory Testing Scheme .....	2
2.2 Description of Materials .....	2
3 Results & Analysis .....	6
3.1 Statistical Evaluation of Results .....	6
3.2 Particle Size Distribution .....	7
3.3 Modified Proctor Compaction .....	10
3.4 Relative Density .....	11
3.5 Specific Gravity .....	12
3.6 Los Angeles Abrasion .....	13
3.7 Resistance Value .....	14
3.8 Direct Shear .....	15
3.8.1 Apparatus and Sample Preparation.....	16
3.8.2 Compacted Density of Direct Shear Samples .....	16
3.8.3 Measured Parameters .....	17
3.8.4 Friction Angle.....	18
3.8.5 Initial Stiffness ( $k_i$ ) Analysis .....	21
3.8.6 Secant Stiffness ( $k_u$ ) Analysis .....	22
3.9 Permeability .....	24
3.9.1 Apparatus .....	24
3.9.2 Sample Preparation .....	26
3.9.3 Testing Procedure .....	27
3.9.4 Results .....	28
3.9.5 Correlation Equations - Background .....	29
3.9.6 Correlation Equations - Results .....	31
3.9.7 Void Ratio-Permeability Relationships .....	34
4 Summary & Conclusions .....	39
5 References.....	41
Appendix A. MDT Grain Size Distribution Analysis Plots .....	43
Appendix B. R-Value Test Reports .....	46
Appendix C. Shear Stress-Displacement Plots .....	61

## LIST OF FIGURES

Figure 1. Location map showing origin of samples.....	3
Figure 2. Pictures of CBC-6A samples from a) Butte, b) Missoula, c) Glendive, d) Billings, e) Great Falls, and f) Kalispell. ....	5
Figure 3. Pictures of CBC-5A samples from a) Missoula, b) Great Falls, and c) Kalispell. ....	5
Figure 4. Pictures of CTS-2A samples from a) Missoula, b) Billings, c) Glendive, d) Lewistown, and e) Havre. ....	5
Figure 5. p-value ranges utilized in this study for the two sample t-test.....	7
Figure 6. MDT specification limits for CBC-5A, CBC-6A, and CTS-2A.....	8
Figure 7. CBC-6A gradation results from the MSU soils lab. ....	8
Figure 8. CBC-5A gradation results from the MSU soils lab. ....	9
Figure 9. CTS-2A gradation results from MSU soils lab.....	9
Figure 10. Comparison of modified Proctor and maximum index densities for CTS-2A. ....	11
Figure 11. Maximum and minimum index density test results. ....	12
Figure 12. R-value test results. ....	15
Figure 13. Direct shear testing apparatus a) mold halves, b) mold placed in load frame with a crane, c) vibratory compactor, and d) assembled mold halves with air bladder and cover plate attached to top.....	16
Figure 14. Void ratio ( $e$ ) for each direct shear test compared to $e_{max}$ and $e_{min}$ . ....	17
Figure 15. Example of strength parameter ( $k_i$ , $k_u$ , and $\sigma_u$ ) determinations. ....	18
Figure 16. Mohr-Coulomb failure envelopes for 6A samples: a) Butte, b) Missoula, c) Glendive, d) Billings, e) Great Falls, and f) Kalispell. ....	19
Figure 17. Mohr-Coulomb failure envelopes for 5A samples: a) Missoula, b) Great Falls, and c) Kalispell. ....	19
Figure 18. Mohr-Coulomb failure envelopes for 2A samples: a) Missoula, b) Billings, c) Glendive, d) Lewistown, and e) Havre.....	20
Figure 19. Internal friction angles ( $\phi'$ ) for each aggregate.....	21
Figure 20. Initial stiffness ( $k_i$ ) results.....	22
Figure 21. Secant stiffness ( $k_u$ ) results. ....	23
Figure 22. Permeameter: a) photograph and b) schematic diagram. ....	25
Figure 23. Support plate for bottom of specimen mold. ....	26
Figure 24. Summary of permeability test results.....	28



---

Figure 25. Calculated permeabilities for the 6A aggregates. ....	32
Figure 26. Calculated permeabilities for the 5A aggregates. ....	33
Figure 27. Calculated permeabilities for the 2A aggregates. ....	33
Figure 28. Void ratio versus permeability for all aggregates in this study. ....	35
Figure 29. Fine fraction void ratio ( $e_f$ ) versus permeability. ....	36
Figure A 1. CBC-6A gradation results from MDT soils lab. ....	44
Figure A 2. CBC-5A gradation results from MDT soils lab. ....	44
Figure A 3. CBC-5A gradation results from MDT soils lab. ....	45
Figure B 1. R-value test report for 2A-Havre. ....	47
Figure B 2. R-value test report for 2A-Glendive. ....	48
Figure B 3. R-value test report for 2A-Missoula. ....	49
Figure B 4. R-value test report for 2A-Lewistown. ....	50
Figure B 5. R-value test report for 2A-Billings. ....	51
Figure B 6. R-value test report for 5A-Missoula. ....	52
Figure B 7. R-value test report for 5A-Kalispell. ....	53
Figure B 8. R-value test report for 5A-Great Falls. ....	54
Figure B 9. R-value test report for 6A-Missoula. ....	55
Figure B 10. R-value test report for 6A-Glendive. ....	56
Figure B 11. R-value test report for 6A-Billings. ....	57
Figure B 12. R-value test report for 6A-Great Falls. ....	58
Figure B 13. R-value test report for 6A-Butte. ....	59
Figure B 14. R-value test report for 6A-Kalispell. ....	60
Figure C 1. Shear stress-displacement plots for 5 psi normal stress: a) 6A samples, b) 5A samples, and c) 2A samples. ....	62
Figure C 2. Shear stress-displacement plots for 10 psi normal stress: a) 6A samples, b) 5A samples, and c) 2A samples. ....	63
Figure C 3. Shear stress-displacement plots for 15 psi normal stress: a) 6A samples, b) 5A samples, and c) 2A samples. ....	64

## LIST OF TABLES

Table 1. Material Specification Limits.....	3
Table 2. Materials Schedule .....	4
Table 3. Sieve Sizes Utilized in this Study.....	7
Table 4. Specific Gravity results.....	13
Table 5. Los Angeles Abrasion Results .....	14
Table 6. Average R-value Statistical Evaluation .....	15
Table 7. Average Internal Friction Angle Statistical Evaluation.....	21
Table 8. Average Initial Stiffness ( $k_i$ ) Statistical Evaluation.....	22
Table 9. Average Secant Stiffness ( $k_u$ ) Statistical Evaluation .....	23
Table 10. Average Permeability Values Based on Aggregate Type.....	29
Table 11. Average Permeability ( $k$ ) Statistical Evaluation .....	29
Table 12. Empirical Permeability Correlation Equations .....	30
Table 13. Ranges of Predicted Permeability Based on Aggregate Type .....	34
Table 14. 1993 AASHTO Minimum Permeability Recommendations .....	37
Table 15. Summary of Key Test Results.....	40

## EXECUTIVE SUMMARY

Highway base courses are typically constructed using crushed and processed aggregate. Roadway designers currently have a number of options for specifying base course material on Montana Department of Transportation (MDT) highway projects. An extensive suite of geotechnical laboratory tests were conducted on 14 different material sources to quantify relative differences in engineering properties of three crushed aggregate types commonly used on MDT highway projects. The material types are identified in the Montana Supplemental Specifications as CBC-6A, CBC-5A, and CTS-2A. The two crushed base course (CBC) materials, CBC-6A and CBC-5A, have maximum particle sizes of 1.5 inches and 2 inches, respectively. The Type A designation indicates that they are untreated. On some projects, a finer-grained leveling course is substituted for the top 0.15 feet of CBC. This leveling course has a smaller maximum particle size and is used in place of CBC at the top of the base course layer to provide a smooth level surface for the placement of asphalt concrete. This study utilized a 0.75-inch maximum particle size material, which is denoted by MDT as crushed top surfacing (CTS) Grade 2 Type A (CTS-2A).

Engineering properties examined in this study included: compaction, durability, strength, stiffness, and drainage. These properties were quantified by synthesizing and analyzing results from the following laboratory tests: geotechnical index tests, direct shear, R-value, and permeability. Multiple repeat tests were conducted on each material. Statistical analyses were performed using the two sample t-test to determine if apparent trends in measured laboratory test results represented true differences between aggregate types.

The CBC-6A aggregates generally exhibited the highest strength and stiffness of the three material types based on R-value tests and direct shear tests on 12-in by 12-in samples. The CBC-6A aggregates exhibited higher  $\phi'$  values and higher R-values than the CTS-2A materials. In terms of strength parameters measured in direct shear testing, there was no statistically significant difference between CBC-5A and CTS-2A materials. The CBC-6A and 5A materials exhibited similar average R-values, which were both slightly greater than the CTS-2A materials. Overall, the CTS-2A materials generally exhibited the lowest average strength and stiffness; however, it still exhibited relatively high strength and stiffness.

Drainage capacity was quantified by conducting multiple saturated constant head permeability tests on 10-inch-diameter samples. The CBC-6A and CTS-2A materials exhibited the highest average permeability ( $k$ ) values, while the CBC-5A materials had the lowest. Permeability was shown to depend more on the fine fraction void ratio ( $e_f$ ) than on aggregate type or maximum particle size. A method of predicting  $k$  based on  $e_f$  was developed, which will allow MDT designers to estimate  $k$  based on gradation and state of compaction. This equation could be useful for comparing the hydraulic properties of base course aggregates, for estimating

hydraulic properties of materials that are out of specification, or to determine the maximum amount of material passing the No. 10 sieve to achieve a particular minimum  $k$ .

Based on results from strength, stiffness, and drainage testing, the CBC-6A materials were generally the best performers in this study. The CBC-5A aggregates generally exhibited the second highest strength and stiffness, but also had the lowest drainage capacity. The CTS-2A aggregates generally exhibited the lowest strength and stiffness, but had relatively good drainage capacity. The ability to substitute CTS-2A material for CBC aggregates depends on the relative importance that is assigned to strength, stiffness, and drainage in the pavement design model.

## 1 INTRODUCTION

Highway base courses are typically constructed using crushed and processed aggregate. Roadway designers currently have a number of options for specifying the base course material on Montana Department of Transportation (MDT) highway projects. The engineering characteristics of these various options have not been thoroughly investigated or quantified by MDT; consequently, the designer must rely on experience and habitual practices. This approach often leads to inconsistencies in design and occasionally misunderstandings between designers, contractors, and materials personnel in regards to aggregate specifications.

The most common options for untreated base course aggregates are described in Section 701.02.4 and Section 701.02.6 of the Montana Supplemental Specifications. These materials are known as crushed base courses (CBC) and crushed top surfacings (CTS). Based on particle size gradations, the three options for untreated base course examined here are: i) CBC Type A Grade 5, ii) CBC Type A Grade 6, and iii) CTS Type A Grade 2. The maximum allowable particle size for Grade 6 and 5 are 1.5 inches and 2 inches, respectively, while CTS Grade 2 has a maximum particle size of 0.75 inches.

The most important engineering characteristics of any base course aggregate are strength, stiffness, and drainage capacity. Each of these properties can have a large impact on the performance of a flexible pavement. For example, increasing the strength and stiffness of the base course results in less rutting, smaller pavement deflections, and ultimately less cracking of the pavement surface. The damaging effects of water in the structural layers of roadways have been well documented. Specific modes of these damaging effects include pumping of fines, frost heave, asphalt stripping, and reduction of shear strength.

The goal of this study is to quantify relative differences in important engineering characteristics of three crushed and processed aggregates. Results from this study will help alleviate confusion among designers and District personnel regarding the use of crushed aggregates, and provide valuable information to construction personnel when faced with requests by contractors to substitute or modify aggregate types.

## 2 METHODS & MATERIALS

### 2.1 Laboratory Testing Scheme

This report summarizes results from laboratory tests that were conducted to quantify physical characteristics of three commonly used crushed and processed aggregates. The primary properties that were examined in this study were: compaction, durability, strength, stiffness, and permeability. These properties were quantified by synthesizing and analyzing results from the following laboratory tests:

- Ø particle size gradation,
- Ø modified Proctor density,
- Ø relative density (maximum and minimum index densities),
- Ø specific gravity,
- Ø Los Angeles abrasion/degradation,
- Ø R-value,
- Ø direct shear, and
- Ø permeability.

### 2.2 Description of Materials

In Montana, untreated base courses generally consist of Crushed Base Course (CBC) aggregates. These CBC aggregates are specified by gradation in Section 701.02.4 of the Montana Supplemental Specifications. As requested by MDT, this study utilized the two most commonly specified base course aggregate gradations: Grade 6 and Grade 5. CBC-6A and CBC-5A aggregates have maximum particle sizes of 1.5 inches and 2 inches, respectively. The Type A designation indicates that they are untreated.

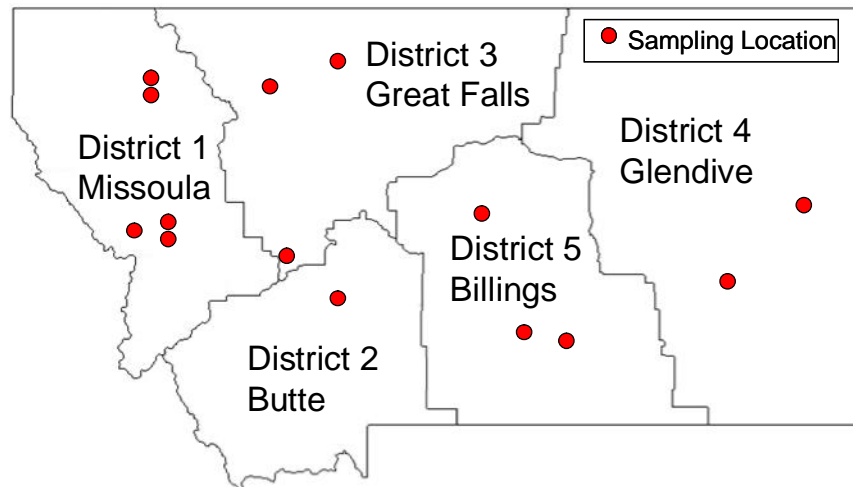
On some projects, a finer-grained leveling course is substituted for the top 0.15 feet of CBC. This leveling course has a smaller maximum particle size and is used in place of CBC at the top of the base course layer to provide a smooth level surface for the placement of asphalt concrete. Aggregates used for this purpose are termed Crushed Top Surfacing (CTS) aggregates, as specified in Section 701.02.6 of the Montana Supplemental Specifications. Like CBC aggregates, CTS aggregates are specified according to gradation. MDT has five different grading options for CTS aggregates. These grading options range from a maximum particle size of 1 inch down to a maximum particle size of 0.375 inch. As requested by MDT, this study utilized the 0.75-inch maximum particle size material, which is denoted by MDT as CTS Grade 2 Type A. The gradation specification limits for the three aggregates used in this study (CBC-6A, CBC-5A, and CTS-2A) are shown in Table 1.

**Table 1. Material Specification Limits**

<b>Sieve Size</b>	<b>CBC-6A</b>	<b>CBC-5A</b>	<b>CTS-2A</b>
2 in		100	
1.5 in	100	94-100	
1 in			
0.75 in	74-96	70-88	100
0.375 in	40-76	50-70	
No. 4	24-60	34-58	40-70
No. 10			25-55
No. 40	6-34	6-30	
No. 200	0-8	0-8	2-8

Note: specification limits are given in percent by weight passing square mesh sieves.

Fifteen different aggregate samples were originally proposed in this study, consisting of five samples of each base course category, each from a different source. The actual number of samples (14) was modified from the prescribed number due to the limited availability of CBC-5A samples. At the time of this study, only three CBC-5A samples were available from MDT. Consequently, an additional CBC-6A sample was added to the testing scheme to keep the total number of samples near the originally prescribed quantity. The modified materials schedule used in this study consisted of a total of fourteen aggregates from a variety of locations across Montana, as shown in Figure 1. Table 2 shows the abbreviations for each material that will be used throughout this report.

**Figure 1. Location map showing origin of samples.**

**Table 2. Materials Schedule**

<b>Aggregate Type</b>		<b>Abbreviation</b>
CBC-6A	Great Falls	6A-Great Falls
	Billings	6A-Billings
	Glendive	6A-Glendive
	Missoula	6A-Missoula
	Butte	6A-Butte
	Kalispell	6A-Kalispell
CBC-5A	Great Falls	5A-Great Falls
	Missoula	5A-Missoula
	Kalispell	5A-Kalispell
CTS-2A	Havre	2A-Havre
	Glendive	2A-Glendive
	Missoula	2A-Missoula
	Lewistown	2A-Lewistown
	Billings	2A-Billings

Visual depictions of 6A, 5A, and 2A aggregates can be seen in Figure 2, Figure 3, and Figure 4, respectively. All photos were taken at approximately the same scale, and a graduated scale in inches is shown at the bottom of each photo. The differences in particle size and gradation between the CBC type aggregates and the CTS type aggregates can be visually discerned by comparing Figure 2, Figure 3, and Figure 4. All aggregates are relatively well graded. The 2A aggregates have a smaller maximum particle size (0.75 inches), while the 5A and 6A aggregates have larger maximum particle sizes (2 and 1.5 inches, respectively). There are also minor visual differences between 5A and 6A aggregates. The 5A aggregates appear to be slightly gap graded with some larger particles and an abundance of sand-size particles, while the 6A aggregates appear to have a better distribution and range of particle sizes.



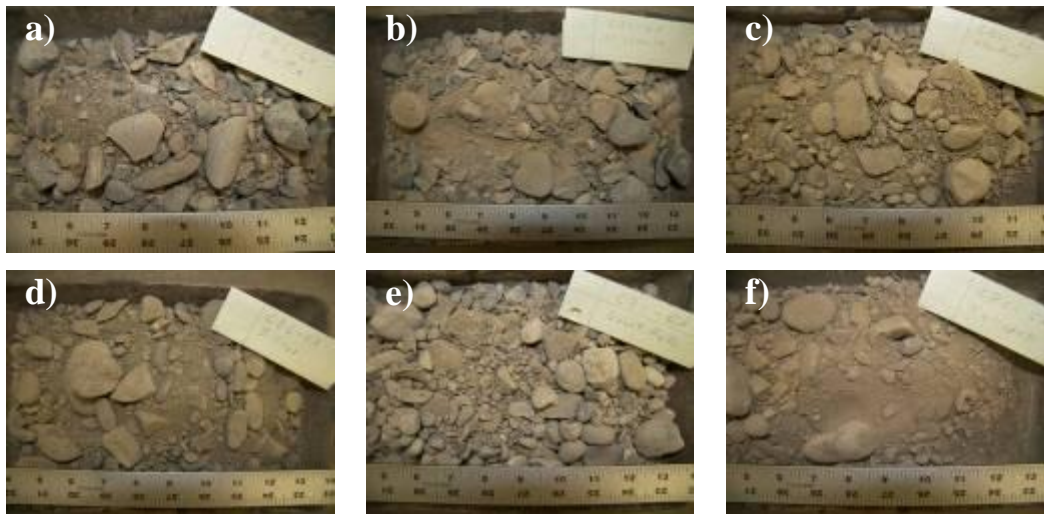


**Figure 2. Pictures of CBC-6A samples from a) Butte, b) Missoula, c) Glendive, d) Billings, e) Great Falls, and f) Kalispell.**



**Figure 3. Pictures of CBC-5A samples from a) Missoula, b) Great Falls, and c) Kalispell.**

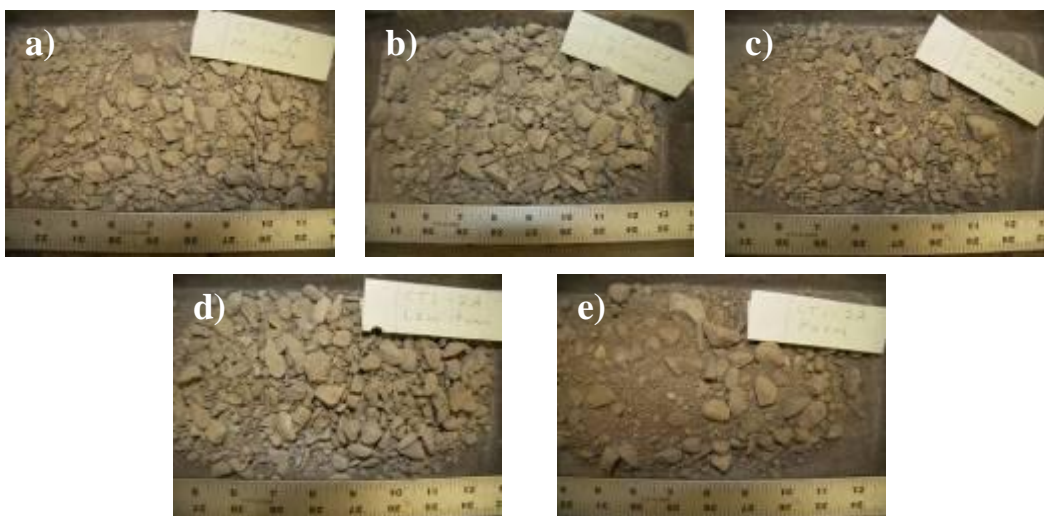


**Figure 4. Pictures of CTS-2A samples from a) Missoula, b) Billings, c) Glendive, d) Lewistown, and e) Havre.**

### 3 RESULTS & ANALYSIS

#### 3.1 Statistical Evaluation of Results

The primary focus of this project is to determine relative differences in important engineering properties between three different aggregate types. Statistical analyses of average values based on aggregate type were conducted using the two sample t-test to determine if apparent trends in measured laboratory test results represent true differences between aggregate types. The following statistical symbols are used throughout this report:

- Ø  $\mu$  = average (also known as the mean),
- Ø  $\sigma$  = standard deviation, and
- Ø COV = coefficient of variation ( $\sigma/\mu$ ).

The two sample t-test is a statistical test used to determine if the averages of two data sets are statistically different based on a mathematical evaluation of data scatter. It can further be used to determine the relationship between the two averages; i.e., whether one average is greater than, less than, or equal to the other. Three separate comparisons are required to determine the relationship between each set of test results (i.e.; 6A versus 5A, 6A versus 2A, and 5A versus 2A).

The output of interest from this statistical test is the p-value parameter, which ranges from 0 to 1 based on the methodology used in this study. Although not typically shown this way, p-values from the t-test can be used to indicate how the two average values compare to each other taking into account data scatter and the number of data points. As shown in Figure 5, p-values between 0 and 0.15 indicate that one average is statistically less than another average; p-values between 0.85 and 1.0 indicate that one average is statistically greater than another average; and p-values between 0.15 and 0.85 indicate the two averages being compared are not statistically different. This may be because the averages are truly the same, or that the standard deviations are relatively large compared to the difference between the averages. In either case, no statistically significant differences can be discerned between the two averages. The two sample t-test does not inherently include cut-off p-values for evaluating the relationship between data sets; rather appropriate cutoff values must be selected by the user. The cut-off p-values of 0.15 and 0.85 were selected by the researchers in this study using judgment based on the relatively large variability that is typically observed in geotechnical test data.

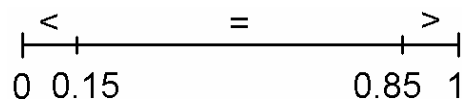


**Figure 5. p-value ranges utilized in this study for the two sample t-test.**

### 3.2 Particle Size Distribution

Grain size analyses were completed on each of the 14 samples in general accordance with AASHTO Test Method T311 and MDT Test Method MT202. Particle size distributions were compared to MDT specified upper and lower gradation limits, which are described in Sections 701.02.4 and 701.02.6 of the Montana Supplemental Specifications. Screen sizes used for gradation analyses were selected based on MDT specifications, as shown in Table 3. Figure 6 shows a comparison plot of the specification limits for the three aggregate types compared in this study.

**Table 3. Sieve Sizes Utilized in this Study**

Sieve Opening (in)	(mm)	Standard Sieve Size
2	50	-
1.5	37.5	-
1	25	-
0.75	19	-
0.5	12.5	-
0.375	9.5	-
0.187	4.75	No. 4
0.079	2	No. 10
0.017	0.425	No. 40
0.003	0.075	No. 200

A dash indicates that a standard sieve size does not exist for this sieve opening size.

Grain size analyses were performed by two separate labs. One set of analyses was performed at the Montana State University (MSU) geotechnical laboratories, and another set was completed by MDT. MSU grain size distributions are shown in Figure 7 through Figure 9, and copies of MDT grain size distributions are provided in Appendix A. Gradation plots compare favorably for the two sets of analyses, with only one notable difference; the MSU gradations show less fine material than the MDT grain size distributions. This is likely due to the fact that the MDT lab performed a wash test on the minus No. 4 size particles, while the MSU lab did not. The slight differences in results could also partially be attributed to variations in methodologies used to fill the multiple sample bags at the source location, and particle segregation that may

occur during sampling, splitting, and testing. In conclusion, the washed test procedure in accordance with MT202 should always be used for particle size analysis.

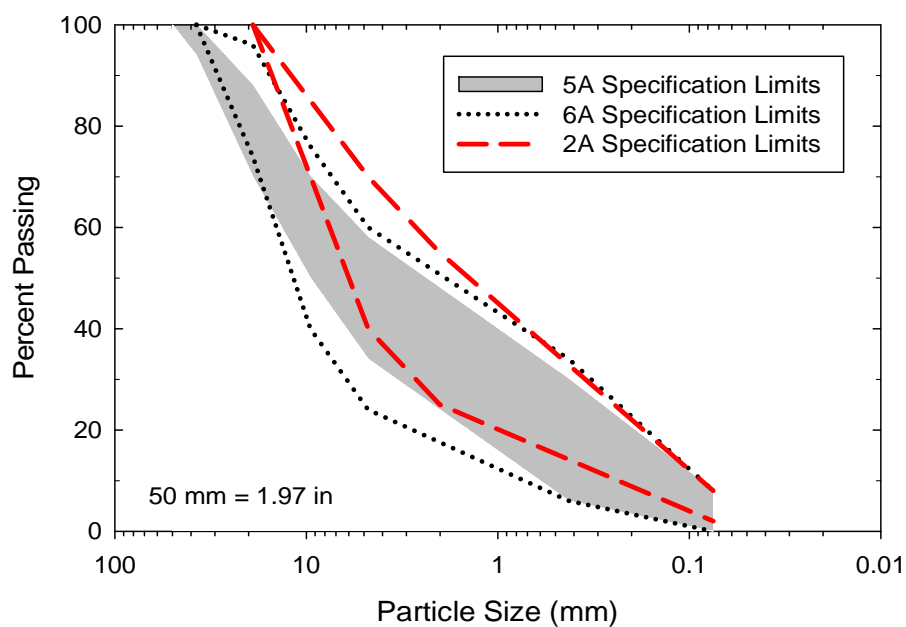


**Figure 6. MDT specification limits for CBC-5A, CBC-6A, and CTS-2A.**

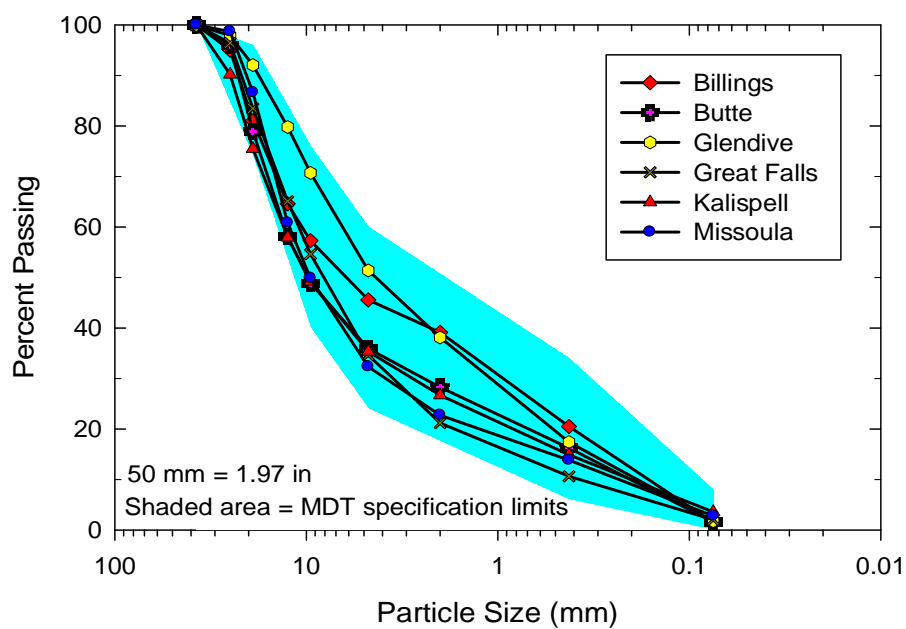
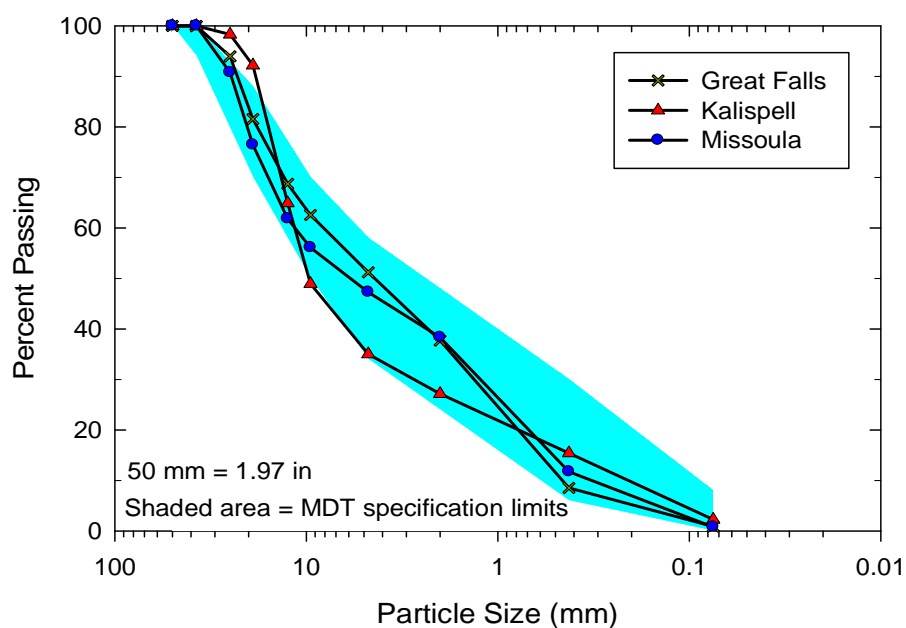


**Figure 7. CBC-6A gradation results from the MSU soils lab.**



### 3.3 Modified Proctor Compaction

Modified Proctor testing was conducted in substantial accordance with MDT Test Method MT230 and general accordance with AASHTO Test Method T180. Because the 2A aggregates had a maximum particle size of 0.75 inches, no screening of oversize particles was necessary with the 6-inch-diameter Proctor mold. Material greater than the 0.75-inch sieve was screened off for testing of the 5A and 6A materials and replaced with an equal weight of material between the No. 4 and 0.75-inch sieve sizes, as specified in MT230. When testing the 5A and 6A materials, several difficulties were encountered in obtaining results that were accurate and repeatable enough for research purposes. These difficulties included excessive amounts of water and fines washing out of the bottom of the Proctor mold, excessive movement of particles when the hammer was applied to the sample, and variations in measured densities depending on the approach used to level-off the top surface of the test specimen. The combined effect of these factors led to inconsistencies in the results. These inconsistencies are generally attributed to the open graded nature of the 5A and 6A aggregates.

ASTM Test Method D2049 specifies that relative index density testing is appropriate for materials with less than 12% passing the No. 200 sieve. In addition, as described in AASHTO Test Methods T99 and T180, the Proctor test is not necessarily applicable for use on cohesionless soils. All aggregate samples evaluated in this study have less than 12% fines and are cohesionless. Consequently, densities obtained from maximum and minimum index density testing (ASTM D4253 and ASTM D4254) were used in place of Proctor densities for evaluating relative densities of prepared samples in this study.

Modified Proctor maximum dry densities for the 2A samples were similar in magnitude to dry densities determined using the maximum index density method, as shown in Figure 10. Density measurements are provided in terms of void ratio ( $e$ ) in Figure 10, which can be related to dry unit weight ( $\gamma_d$ ) using Equation (1), as follows:

$$\gamma_d = \frac{G_s \gamma_w}{1 + e} \quad (1)$$

where,  $G_s$  = specific gravity,  $\gamma_w$  = unit weight of water, and  $e$  = void ratio.

This indicates that either method for determining maximum density would be acceptable for the 2A aggregates. For consistency, maximum dry densities obtained using the maximum index density tests were used in this study for all three aggregate types. It is expected that if accurate Proctor densities could be obtained for 5A and 6A aggregates, they would likely also correspond to maximum dry densities measured using the maximum index density test.

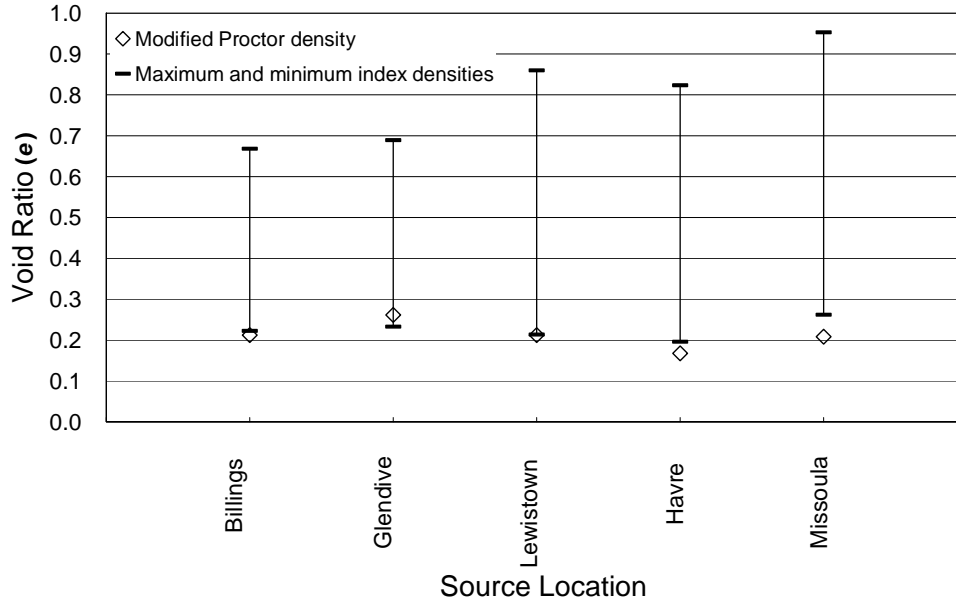


**Figure 10. Comparison of modified Proctor and maximum index densities for CTS-2A.**

### 3.4 Relative Density

Relative density testing was conducted in substantial accordance with ASTM Test Method D4253 (Maximum Index Density and Unit Weight of Soils Using a Vibratory Table) and ASTM Test Method D4254 (Minimum Index Density and Unit Weight of Soils and Calculation of Relative Density). ASTM D4253 provides the option of conducting either dry or saturated testing. It was observed in this study that saturated testing yielded significantly lower minimum void ratios (higher maximum densities) than dry testing. Consequently, all maximum index density results reported herein are based on tests performed under saturated conditions. The size of the mold used for testing was governed by the ASTM specification, which is based on the maximum particle size of the sample. All 2A samples were tested in the 6-inch-diameter (volume = 0.100 ft<sup>3</sup>) mold, while both the 5A and 6A samples were tested in the 10-inch-diameter (volume = 0.500 ft<sup>3</sup>) mold. Relative density can be calculated in terms of either void ratio or dry density as:

$$D_r = \frac{e_{\max} - e}{e_{\max} - e_{\min}} = \left[ \frac{\rho_d - \rho_{d(\min)}}{\rho_{d(\max)} - \rho_{d(\min)}} \right] \left[ \frac{\rho_{d(\max)}}{\rho_d} \right] \quad (2)$$

where,  $D_r$  = relative density,  $e_{\max}$  = maximum void ratio,  $e_{\min}$  = minimum void ratio,  $e$  = in-situ void ratio,  $\rho_d$  = in-situ density,  $\rho_{d(\max)}$  = maximum index density, and  $\rho_{d(\min)}$  = minimum index density.

Maximum and minimum index density results are summarized in Figure 11 in terms of void ratio. This figure shows maximum and minimum void ratios, as well as the associated void ratio

spread ( $e_{max}-e_{min}$ ) for each aggregate. The majority of specimens compacted to a minimum void ratio between 0.20 and 0.25, with three exceptions. The 5A-Kalispell sample had the lowest  $e_{min}$  value (0.17), while the 6A-Missoula and 6A-Glendive samples were on the high end with  $e_{min}$  values of 0.29 and 0.27, respectively.

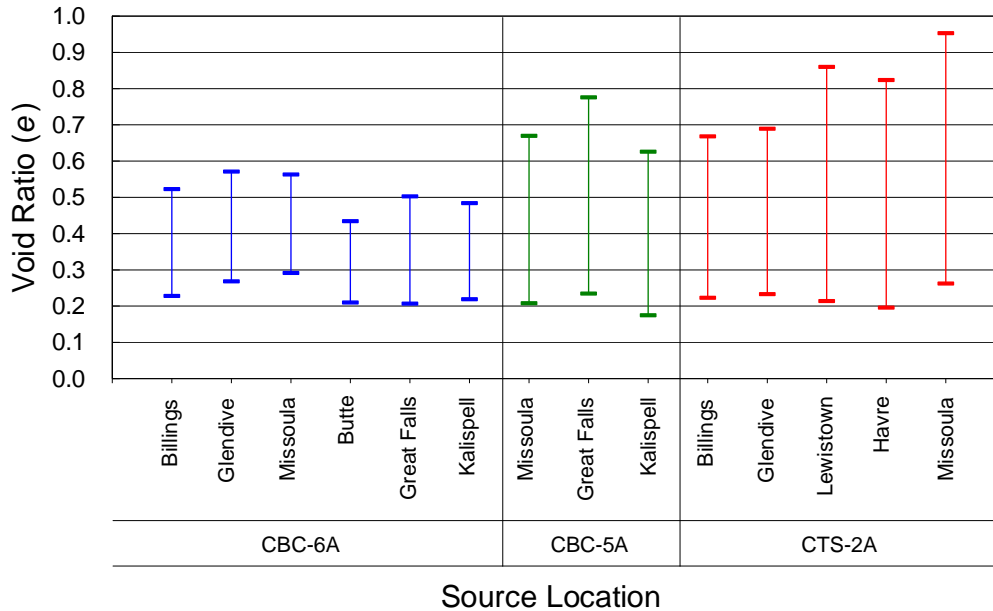


**Figure 11. Maximum and minimum index density test results.**

### 3.5 Specific Gravity

Specific gravity ( $G_s$ ) tests were conducted on the 14 aggregate samples in substantial accordance with MDT Test Methods MT205 (Method of Test for Specific Gravity and Absorption of Coarse Aggregate) and MT220, and general accordance with AASHTO Test Method T85 (Specific Gravity and Absorption of Coarse Aggregate) and AASHTO T100.  $G_s$  was determined by taking a weighted average from the fine and coarse fractions of each soil sample.  $G_s$  values ranging from 2.66 to 2.76 were obtained for the samples tested in this study; well within the typical range reported for these material types (Das 2002).  $G_s$  results are summarized in Table 4.



**Table 4. Specific Gravity results**

<b>Aggregate Type</b>		<b>Specific Gravity</b>
CBC-6A	Great Falls	2.73
	Billings	2.71
	Glendive	2.71
	Missoula	2.72
	Butte	2.68
	Kalispell	2.69
CBC-5A	Great Falls	2.73
	Missoula	2.70
	Kalispell	2.69
CTS-2A	Havre	2.66
	Glendive	2.76
	Missoula	2.76
	Lewistown	2.71
	Billings	2.72

### 3.6 Los Angeles Abrasion

Los Angeles (LA) abrasion tests were conducted in substantial accordance with MDT Test Method MT209 (Resistance to Degradation of Small-Size Coarse Aggregate by Abrasion and Impact in the Los Angeles Machine) and general accordance with AASHTO Test Method T96. LA abrasion tests are used to quantify the relative durability of aggregates. Results from LA abrasion testing are summarized in Table 5. The 2A-Havre and 5A-Missoula samples fell outside of the MDT specification limit of 40 percent loss, with LA abrasion loss percentages of 48.2 and 61.9, respectively. All other samples fell within the MDT specification limit for durability.

The percent loss value for the 2A-Havre sample is about 8 percent greater than the specification limit, and the loss for 5A-Missoula is about 22 percent greater than the limit. It was noted during direct shear testing that the larger particles of the 5A-Missoula sample contained conglomerations of smaller particles that broke apart under load. It is likely that if these conglomerated particles broke apart under load they would also break apart during repeated impact. Consequently, it is hypothesized that the high loss percentage exhibited by this sample is a result of the tendency of the larger conglomerated particles to break apart during impact.

**Table 5. Los Angeles Abrasion Results**

Aggregate Type		Percent Loss
CBC-6A	Great Falls	27.3
	Billings	23.5
	Glendive	22.3
	Missoula	15.3
	Butte	19.0
	Kalispell	15.5
CBC-5A	Great Falls	19.0
	Missoula	61.9
	Kalispell	13.2
CTS-2A	Havre	48.2
	Glendive	15.3
	Missoula	13.1
	Lewistown	24.1
	Billings	16.9

### 3.7 Resistance Value

The Resistance R-value and Expansion Pressure of Compacted Soils test (commonly referred to as the R-value test) is used by MDT to evaluate the strength and stability of subgrade and base materials. The test is standardized by AASHTO Test Method T190 and ASTM Test Method D2844. The R-value test output is a number ranging from 0 to 100, with 0 representing viscous liquid slurry with no shear resistance, and 100 representing a rigid solid. The R-value test is conducted using a stabilometer, in which a constant vertical pressure is added to the stabilometer and the corresponding increase in horizontal (fluid) pressure is measured. The R-value is calculated based on the measure of horizontal pressure increase.

R-value tests were completed by MDT at their Helena materials testing lab. R-value results are summarized in Figure 12, and data sheets for the R-value tests are provided in Appendix B. All soils in this study are classified as A-1-a in the AASHTO soil classification system. Published correlations suggest that R-values for A-1-a soils would likely range from approximately 70 to greater than 80 (PCA 1966, Van Til et al. 1972). As shown in Figure 12, slight differences in average R-values were observed between the different aggregate types. A series of two sample t-tests were performed to determine if differences in the average values are statistically significant. Results from this statistical evaluation are shown in Table 6. Based on the statistical testing, the average 2A R-value (66.6) was less than both the average 6A R-value (74.5) and the average 5A R-value (72.0). There is no statistically significant difference between the average 6A and average 5A R-values. From a practical viewpoint, the relative differences are not significant based on the accuracy of the test.

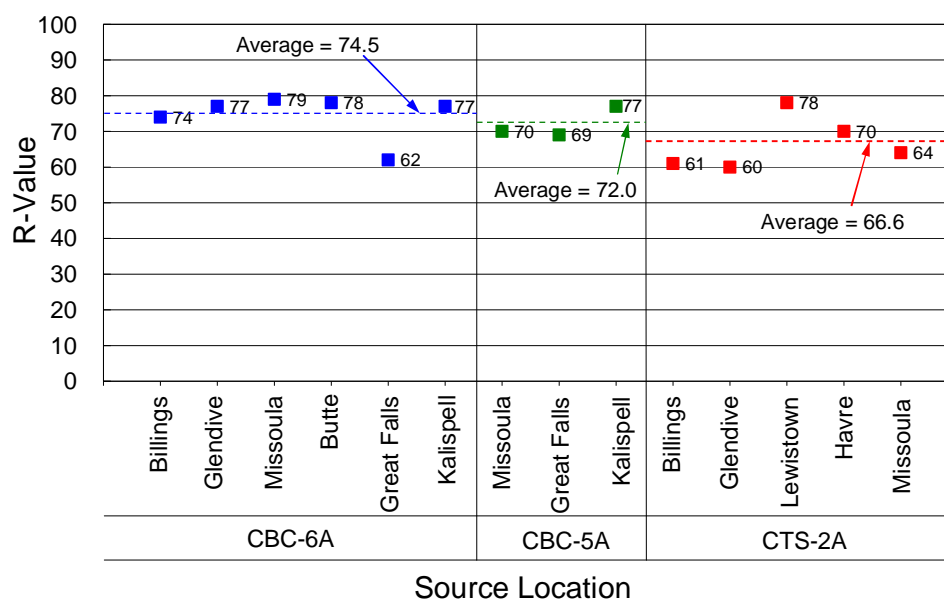


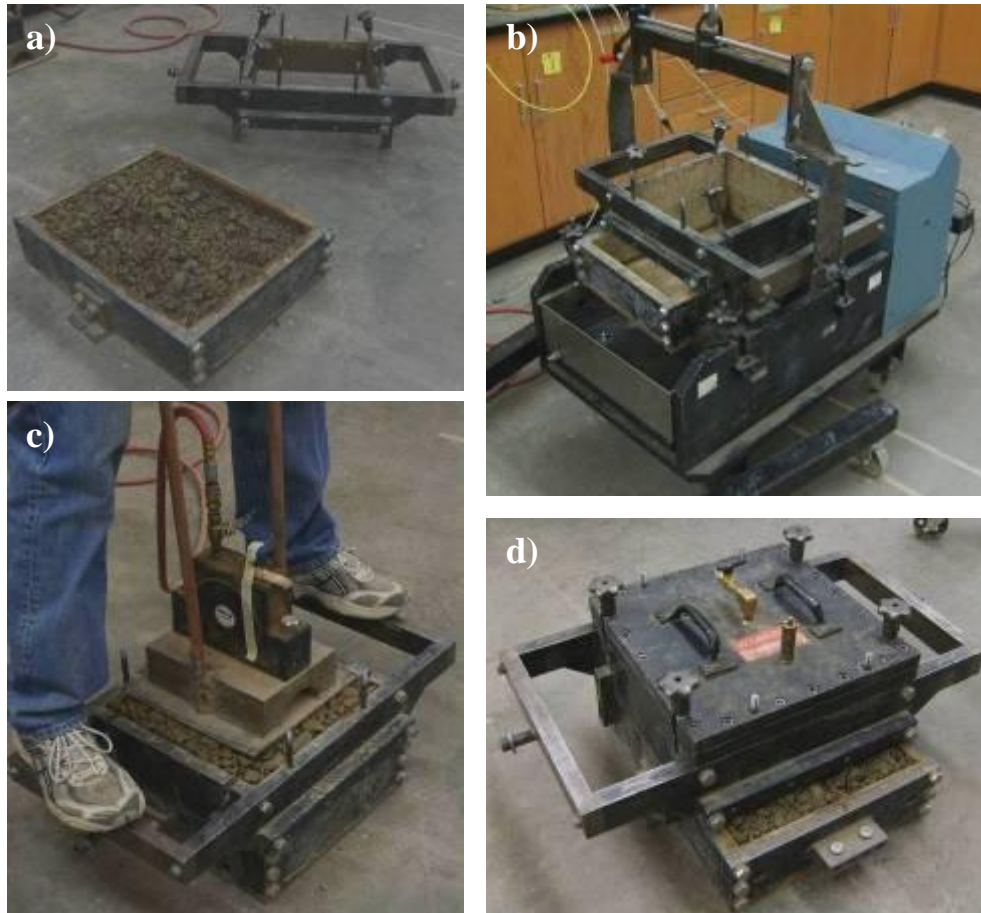
Figure 12. R-value test results.

Table 6. Average R-value Statistical Evaluation

Relationship		p-value
6A $\mu=74.5$	= 5A $\mu=72.0$	0.740
6A $\mu=74.5$	> 2A $\mu=66.6$	0.950
5A $\mu=72.0$	> 2A $\mu=66.6$	0.873

### 3.8 Direct Shear

Direct shear testing was performed to quantify shear strength parameters of the aggregate samples. Tests were performed in general accordance with AASHTO Test Method T236. A large 12-inch by 12-inch Brainard-Kilman direct shear testing apparatus was used to accommodate the maximum particle size of the aggregate samples. Shear resistance was measured using an S-type load cell and lateral displacement was measured using a linear variable displacement transducer (LVDT). Figure 13 shows some of the main components of the direct shear device.



**Figure 13. Direct shear testing apparatus a) mold halves, b) mold placed in load frame with a crane, c) vibratory compactor, and d) assembled mold halves with air bladder and cover plate attached to top.**

### 3.8.1 Apparatus and Sample Preparation

Soil was placed into the shear box in 1.3-inch compacted lifts. Compaction was performed at 4 percent moisture using a 57 pound pneumatic vibratory compactor with a 100 in<sup>2</sup> contact area (Figure 13c). Normal stress (pressure) was applied to the sample using a pressurized rubber air bladder, which was located on the inside of the shear box lid (Figure 13d). The samples were sheared at a constant rate of 0.05 in/min to a maximum horizontal displacement of 3.8 inches. The horizontal displacement rate was slow enough to ensure full drainage (effective stress conditions).

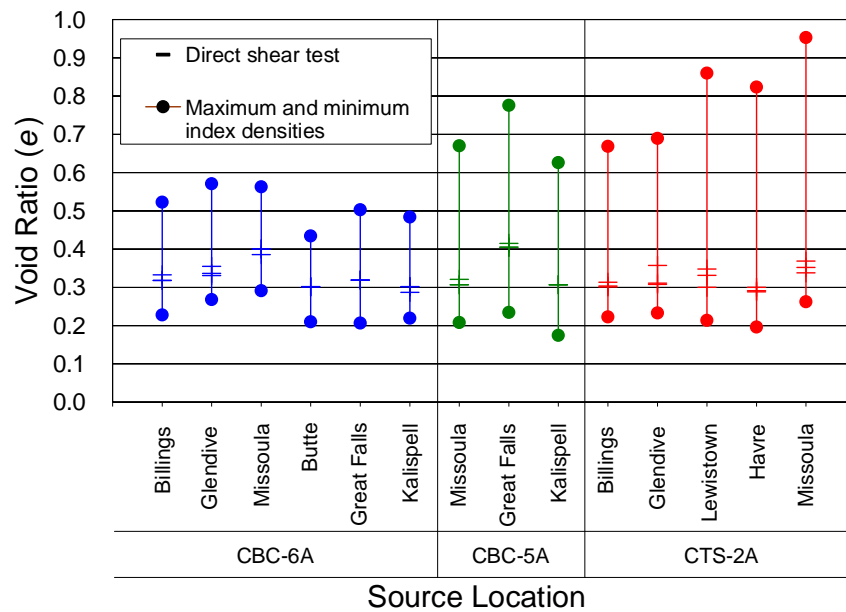
### 3.8.2 Compacted Density of Direct Shear Samples

In the field, large vibratory drum compactors pass over a material multiple times to impart weight and vibration to the underlying geomaterials. This process was simulated in the laboratory using a weighted vibratory plate. Vibration and impact compaction energy were applied until observable particle movement ceased, which generally occurred after

approximately 1 minute of compaction for each soil layer. This method of compaction provided high densities with minimal compaction non-uniformities. All samples were compacted using an initial water content of 4% to help minimize particle segregation.

The dry density of the direct shear samples was determined using mass-volume relationships after each sample was compacted into the direct shear mold. Relative density ( $D_r$ ) was calculated for each compacted sample using Equation (2).

There is some variation in  $D_r$  between aggregate types because of the differences in particle gradation, particle shape, and maximum particle size. Overall, good repeatability was achieved using this method of compaction, as evidenced by the relatively small spread of compacted void ratios, as shown by the dashed symbols in Figure 14.



\* If less than 3 void ratios are displayed for each sample, some of them overlap.

**Figure 14. Void ratio ( $e$ ) for each direct shear test compared to  $e_{max}$  and  $e_{min}$ .**

### 3.8.3 Measured Parameters

Several parameters were obtained from direct shear testing including initial stiffness ( $k_i$ ), ultimate secant stiffness ( $k_u$ ), and ultimate strength ( $\sigma_u$ ). Mohr-Coulomb failure envelopes were determined from the ultimate strength of each material at different normal stresses. Values of  $k_i$  reported here are defined as the slope of the linear elastic portion of the stress-displacement curve, which occurs at low displacements.  $k_u$  is defined as the slope of a line drawn from the origin to the shear stress at 8% strain, where the strain is averaged over the entire length of the sample. Percent strain in this context is thus defined as the measured displacement divided by sample width.  $\sigma_u$  was determined at 8% strain or the peak stress, whichever occurred first. An example illustrating how these values were determined for the 6A-Missoula, 10 psi sample, is

shown in Figure 15. Shear stress versus horizontal displacement plots for all three normal stresses are provided in Appendix C for each material.

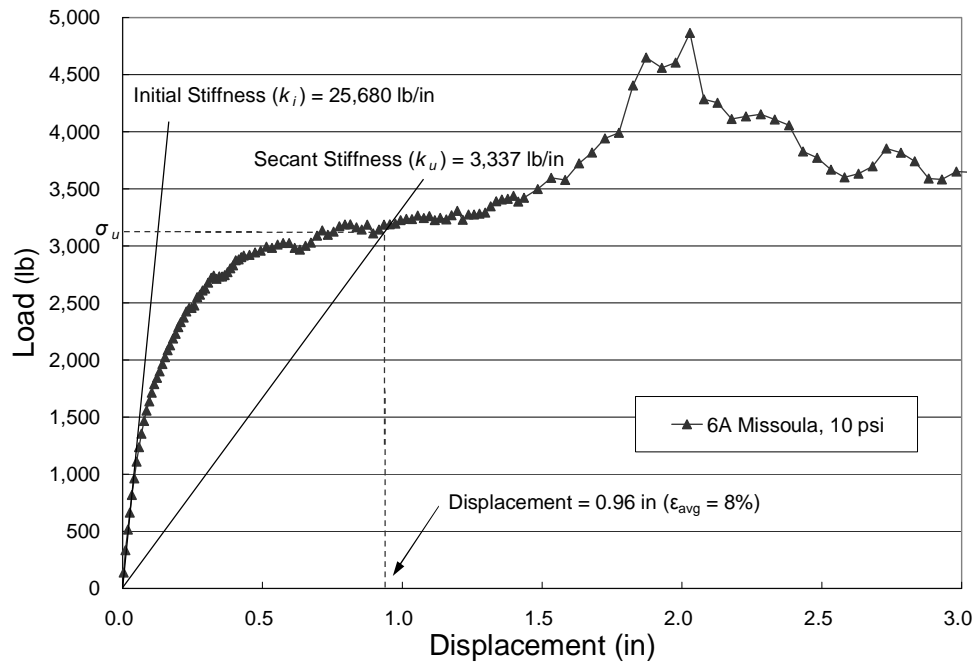


**Figure 15. Example of strength parameter ( $k_i$ ,  $k_u$ , and  $\sigma_u$ ) determinations.**

### 3.8.4 Friction Angle

The effective angle of internal friction ( $\phi'$ ) was determined by testing three separately compacted samples (each with virgin material) at normal stresses of 5, 10, and 15 psi. In the field, these aggregates likely experience relatively low normal stresses because of the small overburden loads that are typical of highway pavement sections. Normal pressures of 5, 10, and 15 psi were used to simulate the low normal pressures typical of in-situ conditions. The spread of 5 psi between normal pressures is a practical measure necessary to provide accurate Mohr-Coulomb failure envelopes. Mohr-Coulomb failure envelopes are presented in Figure 16, Figure 17, and Figure 18 for the 6A, 5A, and 2A samples, respectively. Effective friction angles shown in the plots are based on best fit lines drawn through the origin.

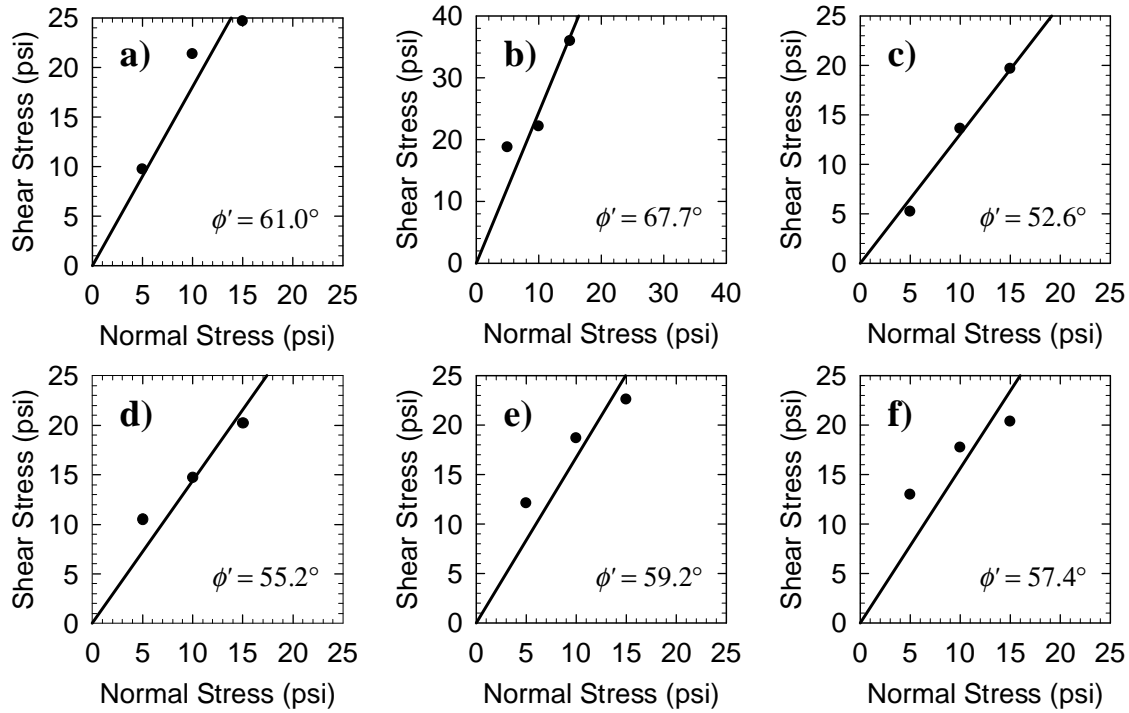


**Figure 16. Mohr-Coulomb failure envelopes for 6A samples: a) Butte, b) Missoula, c) Glendive, d) Billings, e) Great Falls, and f) Kalispell.**

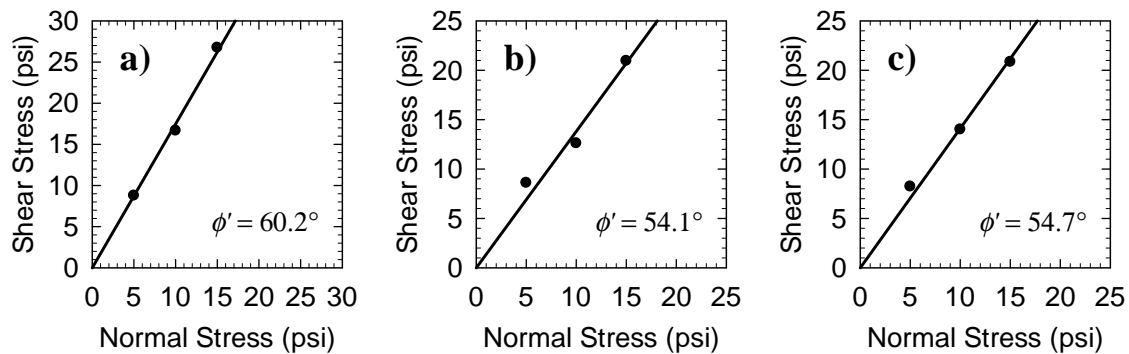


**Figure 17. Mohr-Coulomb failure envelopes for 5A samples: a) Missoula, b) Great Falls, and c) Kalispell.**

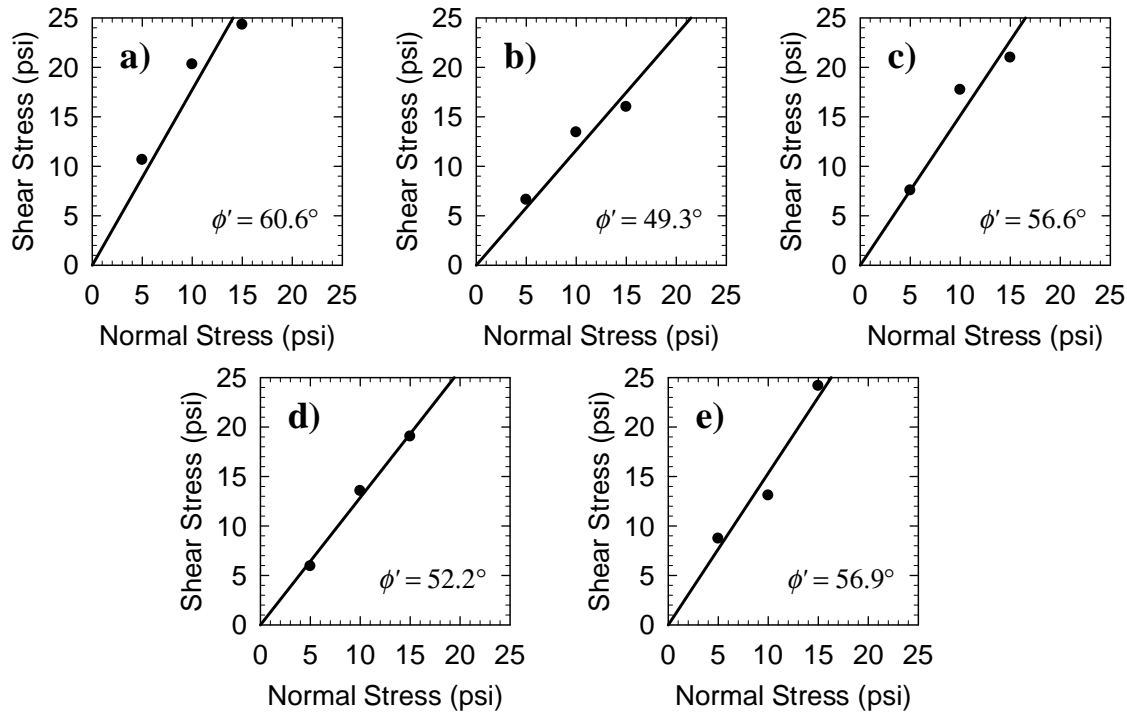


**Figure 18. Mohr-Coulomb failure envelopes for 2A samples: a) Missoula, b) Billings, c) Glendive, d) Lewistown, and e) Havre.**

Measured  $\phi'$  values were in the range of 49° to 68°, which represents a relatively large spread. Figure 19 provides a direct comparison of  $\phi'$  values for the three aggregate types. A series of two sample t-tests were performed on the average  $\phi'$  values to determine the statistical significance of the scatter or spread in results. The results of this statistical evaluation are summarized in Table 7, which indicates that the average 6A effective friction angle (58.8°) is larger than the average 2A friction angle (55.1°). When the spread of data is taken into account, there is not a significant difference in the  $\phi'$  values between the 6A and 5A materials or between the 5A and 2A materials.



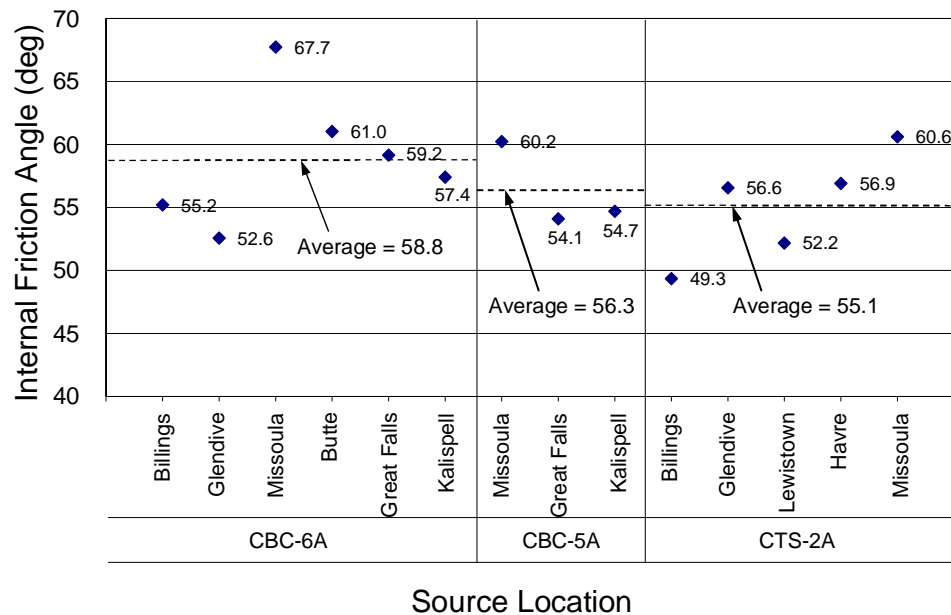


**Figure 19. Internal friction angles ( $\phi'$ ) for each aggregate.**

**Table 7. Average Internal Friction Angle Statistical Evaluation**

Relationship			p-value
6A	=	5A	0.791
$\mu=58.8$		$\mu=56.3$	
6A	>	2A	0.882
$\mu=58.8$		$\mu=55.1$	
5A	=	2A	0.660
$\mu=56.3$		$\mu=55.1$	

### 3.8.5 Initial Stiffness ( $k_i$ ) Analysis

Failure of roadway materials is generally defined by relatively small deformations, which are related to the initial portion of the stress-displacement curve.  $k_i$  is defined as the slope of the stress-displacement curve at low displacements, where the curve is relatively linear, as exemplified in Figure 15.

Values of  $k_i$  for all of the samples tested are compared in Figure 20. These values generally ranged from 10,000 lb/in to 30,000 lb/in. As expected, most aggregates exhibited increasing  $k_i$  with increasing normal stress. There were some minor exceptions to this trend, which may be attributed to small variations in the test pressures and variations in sample collection methodology, compaction non-uniformities, and minor particle segregation during sampling and sample preparation.

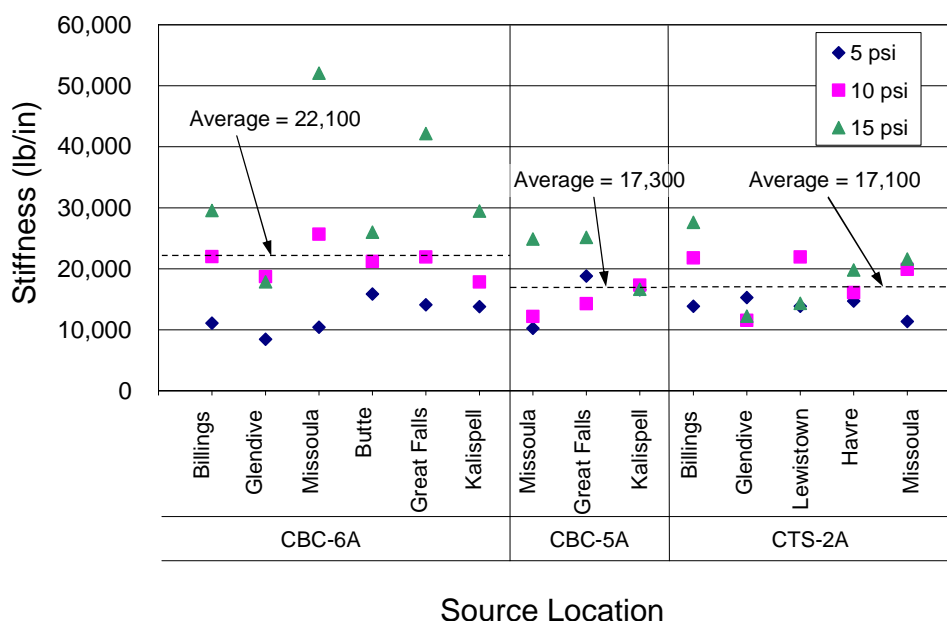


**Figure 20. Initial stiffness ( $k_i$ ) results.**

A series of two sample t-tests were performed to determine if the apparent trends in average  $k_i$  values were statistically significant. The results of the statistical evaluation are summarized in Table 8. The average  $k_i$  of the 6A aggregate type (22,100 lb/in) is statistically greater than the average  $k_i$  of the 2A aggregate type (17,100 lb/in) and the 5A aggregate type (17,300 lb/in). There is no significant difference between the average  $k_i$  of the 5A and 2A aggregate types.

**Table 8. Average Initial Stiffness ( $k_i$ ) Statistical Evaluation**

Relationship			p-value
6A	>	5A	0.931
$\mu=22.1$		$\mu=17.3$	
6A	>	2A	0.953
$\mu=22.1$		$\mu=17.1$	
5A	=	2A	0.552
$\mu=17.3$		$\mu=17.1$	

### 3.8.6 Secant Stiffness ( $k_u$ ) Analysis

Secant stiffness ( $k_u$ ) values were determined for each aggregate to evaluate the soil behavioral characteristics at large strains.  $k_u$  is defined here as the slope of a line drawn from the origin to the shear stress at 8% strain on a shear stress-displacement curve, as shown in Figure 15.  $k_u$  may not be as relevant as  $k_i$  because roadway base course aggregates could only experience 8% strain during a major shear failure, which would not be typical. However,  $k_u$  is a

meaningful parameter that can be used for quantifying strength and stiffness differences between different aggregates.

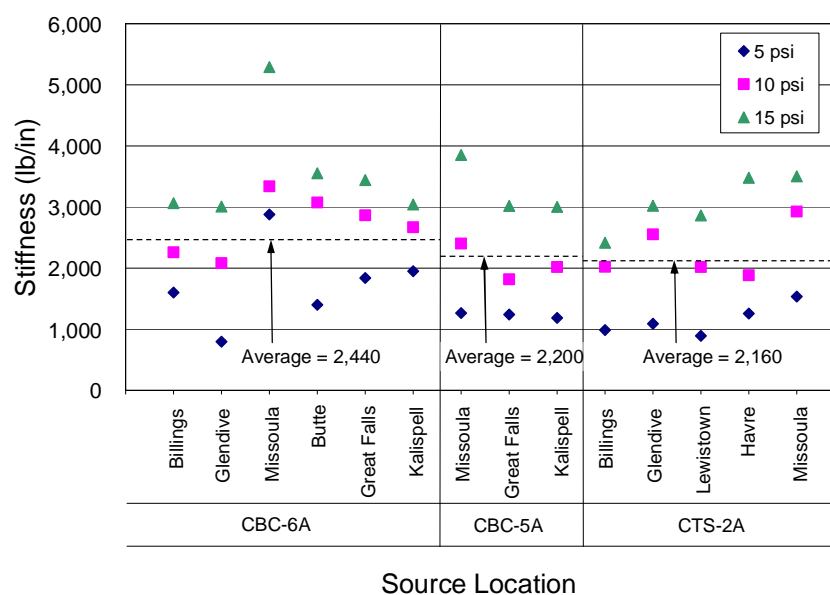


**Figure 21. Secant stiffness ( $k_u$ ) results.**

As shown in Figure 21,  $k_u$  values generally ranged from 1,000 lb/in to 3,500 lb/in. All aggregates exhibited increasing  $k_u$  values with increasing normal stresses. The 6A-Missoula sample exhibited significantly higher secant stiffness than all of the other samples. A series of two sample t-tests were performed to compare average  $k_u$  values based on aggregate type. Results of this statistical evaluation are presented in Table 9.

**Table 9. Average Secant Stiffness ( $k_u$ ) Statistical Evaluation**

Relationship			p-value
6A	>	5A	0.878
$\mu=2.44$		$\mu=2.20$	
6A	>	2A	0.934
$\mu=2.44$		$\mu=2.16$	
5A	=	2A	0.538
$\mu=2.20$		$\mu=2.16$	

The average  $k_u$  of the 6A aggregate type (2,440 lb/in) is greater than the average of the 2A aggregate type (2,160 lb/in) and the 5A aggregate type (2,200 lb/in). There is no significant difference between the average  $k_u$  of the 5A and 2A aggregates. This indicates that at relatively large displacements, these aggregates all exhibit relatively similar stress-displacement behavior, with the 6A aggregate type exhibiting only a small potential advantage over the other aggregates. Trends observed in the  $k_u$  results are similar to the  $k_i$  results.

### 3.9 Permeability

Drainage capacity of the aggregates was quantified by conducting saturated constant head hydraulic conductivity (permeability) tests. Permeability tests were performed in general accordance with ASTM Test Method D2434 and AASHTO Test Method T215 (Permeability of Granular Soils - Constant Head). Constant head testing was utilized (as opposed to falling head) to limit the amount of hydraulic head applied to the samples thus ensuring laminar flow conditions. Darcy's Law was used to compute permeability, as follows:

$$k = \frac{QL}{tHA} \quad (3)$$

where,  $k$  = permeability,  $Q$  = volume of water passed through the specimen,  $L$  = length of the specimen,  $t$  = elapsed time corresponding to  $Q$ ,  $H$  = total head across the specimen, and  $A$  = cross sectional area of the specimen perpendicular to the flow direction.

Permeability is a highly variable soil property that can vary significantly with small variations in compaction and gradation. To minimize testing errors, average  $k$  values were obtained for each sample by conducting three separate tests, using virgin aggregate each time. The experimental results were compared to empirical estimation equations and published typical ranges.

#### 3.9.1 Apparatus

A custom-built large-diameter permeameter was utilized for this testing. The permeameter specimen mold has a diameter of 10 inches and an approximate height of 10 inches. The permeameter utilizes a unique Mariotte tube and integral upper reservoir arrangement to maintain constant pressure head and complete saturation of the soil sample and testing apparatus throughout the experiment. A photograph and schematic diagram of the permeameter are shown in Figure 22.

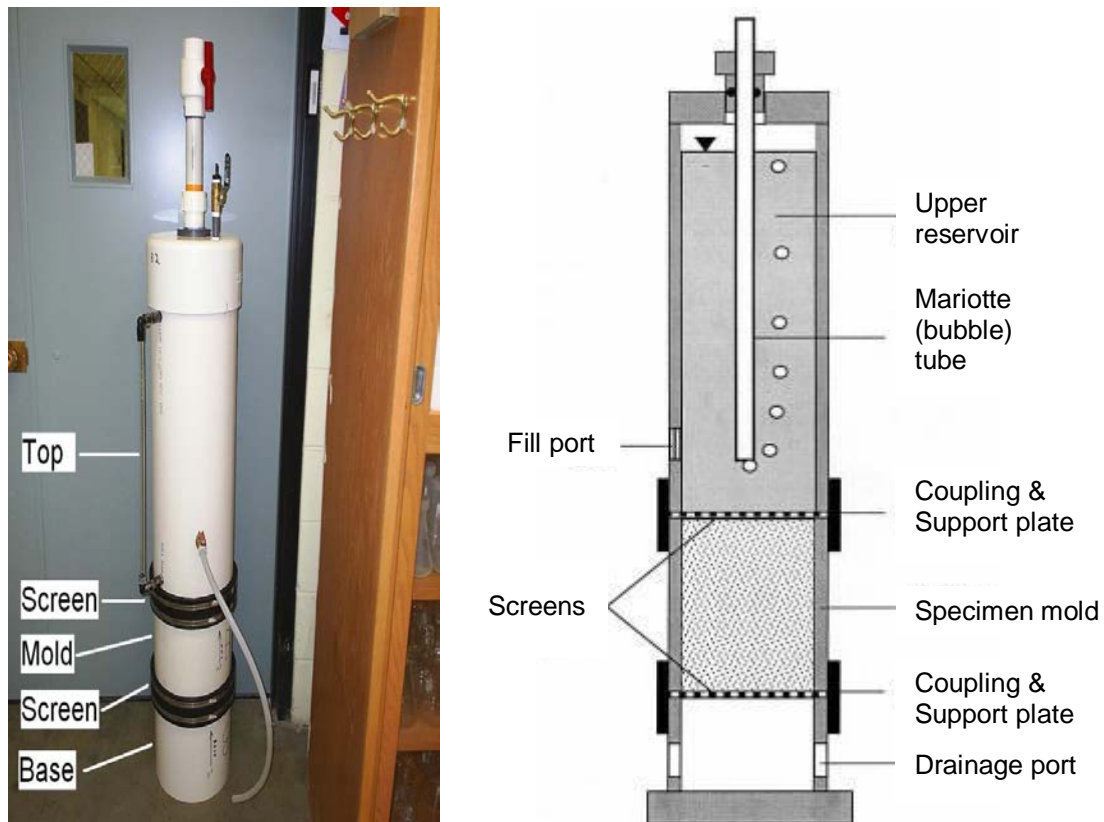


**Figure 22. Permeameter: a) photograph and b) schematic diagram.**

There are several notable improvements in this custom-built device over a traditional constant head permeability testing apparatus. The apparatus used in this study completely submerges the specimen in the tail water tank, which ensures the specimen remains saturated throughout the test. There is no head loss between the head water tank and specimen because there are no tubes, valves, or fittings between the headwater and specimen. Only a screen and support plate separates the supply water from the specimen. The upper reservoir is used to supply water to the sample and can be precisely measured using a manometer, which eliminates the need to collect and measure the tail water. Additionally, the use of a Mariotte tube to maintain constant head eliminates the waste of overflow head water, which is inherent in traditional permeameter devices.

The specimen support plates are shown in Figure 23. The support plates consist of 0.25 in thick galvanized steel plates that have 0.25 in holes throughout to permit unrestricted flow of water. Two square mesh screens, oriented at 45° relative to each other, were placed between the sample and the support plates to reduce the washing of finer particles out of the specimen during testing. The screens were placed at 45° relative to each other to further reduce the opening size of the sieves, thereby reducing the movement of fines.



**Figure 23. Support plate for bottom of specimen mold.**

A 0.125-inch thick soft neoprene rubber liner with 450 psi tensile strength and 10A durometer hardness was attached to the inside of the specimen mold with silicone adhesive to reduce edge effects, as suggested by Thornton and Toh (1995). The liner was installed to alleviate high stress concentrations that may occur at the contact points of the larger particles on the smooth rigid interior wall of the mold, and to maintain a more uniform and representative distribution of particles near the sample edges. The liner was used for all tests performed in this study. Any effect imparted on the measured permeability from the presence of the liner was approximately the same for all samples.

### 3.9.2 Sample Preparation

Samples of virgin aggregate were compacted into the 10-inch tall specimen mold in five lifts using 15 drops from a modified Proctor hammer (with a 10-lb weight and 18-inch drop). Relatively low energy was utilized for compaction ( $2,600 \text{ lb-ft/ft}^3$ ) to avoid damaging the bottom screens. Impact was selected as the compaction mechanism to minimize particle segregation. For consistency, all samples were compacted at an initial water content of 4%.

Preventing particle segregation during placement and compaction is particularly important in permeability testing because a non-homogenous distribution of the finer sized particles can have a large effect on the measured permeability (Moulton 1980). In addition, careless sample preparation and compaction techniques can lead to inaccurate results. Even if extreme care is taken, the measured value of permeability may likely only be within one order of magnitude of the true value (Bowles 1992). Every effort was made in the preparation, placement, and compaction of samples to minimize particle segregation and to ensure consistency between test specimens.

Sample preparation consisted of compacting the aggregate in layers in the permeameter mold, placing the screens in the proper orientation, and saturating the samples and apparatus.

Approximately 35 to 40 gallons of water were prepared for each test. This included water for filling the tail water container, saturating the sample, and filling the upper reservoir. Partially de-aired water was used to minimize potentially adverse effects of air bubbles in the system during saturation and testing. The use of 100% de-aired water was not practical in this study because of the large quantity of water used in each test. It is postulated that the small amount of entrapped air in the test water would have had only minor influences on the *absolute* results and no influence on the *relative* difference between results because identical procedures were used to prepare each sample.

A small negative pressure (vacuum) was applied to the reservoir tube to draw in head water and to help saturate the soil specimen. While applying the vacuum through the vacuum port at the top of the reservoir tube, the side port was opened to allow water to fill the upper reservoir. This created a slight negative hydraulic gradient across the sample thereby causing water to be drawn up through the specimen. The vacuum forced entrapped air bubbles out of the sample and consequently enhanced the saturation process. The negative pressure was kept small to avoid washing fines from the specimen into the upper reservoir. Samples were filled under low vacuum at a rate of approximately 0.6 gal/min. This slow filling rate and low vacuum was selected to provide a balance between the removal of air bubbles and the control of fines migration.

### 3.9.3 Testing Procedure

After the sample is fully saturated, the upper reservoir is attached to the specimen mold and filled with water. The procedure for filling the reservoir and running a test is outlined below:

- Ø Install the upper reservoir using the coupling near the top of the specimen mold and adjust the height of the Mariotte tube to control the hydraulic gradient through the sample.
- Ø Open the side port and the vacuum port.
- Ø Plug the top of the Mariotte tube.
- Ø Apply a small amount of vacuum to the vacuum port. This will draw water into the side port from the tailwater tub. Leave vacuum on until the upper reservoir is completely full of water. Additional water will need to be added to the tailwater tub as it is drawn into the upper reservoir.
- Ø Close the vacuum and side ports after the upper reservoir is completely filled with water.
- Ø Unplug the Mariotte tube to initiate the flow of water through the sample.
- Ø Allow the system to approach steady state conditions.
- Ø Record the water level and *start* time.
- Ø Record the water level and *stop* time just before the water reaches the bottom of the Mariotte tube.

ASTM D2434 and AASHTO T215 suggest that permeability testing should not be started until the system completely reaches steady state conditions. However, for the wide range of particle sizes examined in this study, it was observed that running excessively large quantities of water through the specimen before testing is started could be counter-productive. Excessive seepage, especially at high gradients could change the results of the test because fines could be washed out of the specimen. It was determined that using a carefully controlled hydraulic gradient and a water volume of 2.3 gallons allowed the system to approach steady state successfully because generally only minor changes in permeability were noted after this initial volume of water drained through a sample.

Relatively low hydraulic gradients were used on all samples to ensure that the assumptions inherent in Darcy's Law were not violated and to provide consistency between tests. ASTM D2434 recommends applying gradients of 0.2 to 0.3 ft/ft to coarse grained soils and gradients of 0.3 to 0.5 ft/ft to finer soils. All of the aggregate samples examined in this study were predominately coarse-grained; consequently, a hydraulic gradient of 0.26 ft/ft was used.

### 3.9.4 Results

Saturated permeabilities were determined for each aggregate in this study by conducting three independent permeability tests (each using virgin aggregates). Permeability results for each test are summarized in Figure 24, and average results for each aggregate type are shown in Table 10. The COV values shown in Table 10 are relatively large, which is attributed to the inherently highly variable nature of this parameter. (Values of  $k$  are presented in this section using units of cm/s as is typical practice in the United States. Whenever practically possible, US Customary units are also presented.)

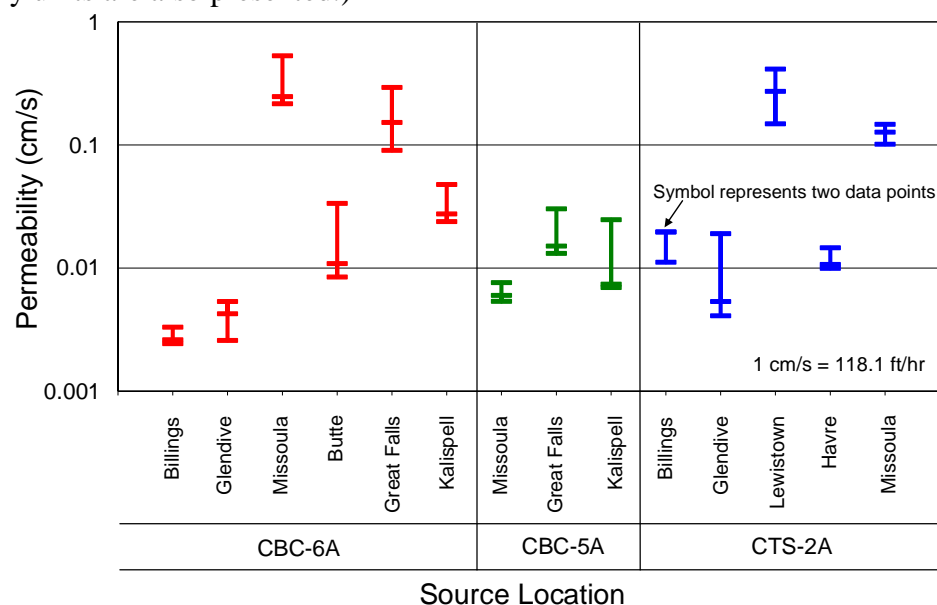


**Figure 24. Summary of permeability test results.**



**Table 10. Average Permeability Values Based on Aggregate Type**

Aggregate Type	Average $k$		Standard Deviation, $\sigma$		COV
	(ft/hr)	(cm/s)	(ft/hr)	(cm/s)	
6A	11.1	0.094	16.9	0.143	1.52
5A	1.5	0.013	1.1	0.009	0.69
2A	10.4	0.088	14.2	0.120	1.36

A series of two sample t-tests were performed to facilitate the evaluation of average permeability values. The results of this statistical evaluation are presented in Table 11. The average permeabilities for each aggregate type were all in the same order of magnitude, ranging from 0.094 to 0.013 cm/s (11.1 to 1.5 ft/hr). The statistical evaluation indicates that 6A and 2A aggregates both have higher average permeabilities than the 5A aggregates. There is no statistically significant difference between the average permeabilities of the 2A and 6A samples.

**Table 11. Average Permeability ( $k$ ) Statistical Evaluation**

Relationship			p-value
6A $\mu=11.1$	>	5A $\mu=1.5$	0.986
6A $\mu=11.1$	=	2A $\mu=10.5$	0.552
5A $\mu=1.5$	<	2A $\mu=10.5$	0.015

The measured permeability values fell within typical reported ranges based on general soil type. Measured values of permeability for the aggregates in this study varied from 0.003 to 0.50 cm/s (0.35 to 59.1 ft/hr), similar to the range reported by Holtz and Kovacs (1981) for clean sands and gravels 0.001 to 1.0 cm/s (0.12 to 118.1 ft/hr).

### 3.9.5 Correlation Equations - Background

Published correlation equations were also utilized to further examine the reasonableness of the measured permeability values and to explore the potential usefulness of empirical relationships. These equations rely on data obtained from geotechnical index testing to estimate the permeability of a soil. Although the parameters used to determine permeability vary from equation to equation, they generally rely on particle size and/or void space measurements of the soil. Table 12 summarizes the six empirical equations that were evaluated using data measured in this study.

**Table 12. Empirical Permeability Correlation Equations**

Author	Year	Equation	Test Validity
Hazen	1911	$k = C_H d_{10}^2$	Sands between 0.1 and 3.0 mm
Terzaghi	1925	$k = \frac{C}{\mu_o} \frac{\mu_o}{\mu_T} \left[ \frac{n - 0.13}{(1 - n)^{1/3}} \right]^2 d_{10}^2$	Sands with non-uniform grain size and shape
Moulton	1980	$k = \frac{0.00219 * 10^5 (d_{10})^{1.478} n^{6.654}}{(P_{200})^{0.597}}$	Roadway subbase aggregates
Shahabi et al.	1984	$k = 1.2 C_u^{0.735} d_{10}^{0.89} \frac{e^3}{1 + e}$	Medium to fine sand
Chapuis	2004	$k = 2.4622 \left[ d_{10}^2 \frac{e^3}{1 + e} \right]^{0.7825}$	Saturated sands and gravels
Chapuis	2004	$k = \frac{C_H d_{10}^2 e^3 (1 + e_{\max})}{e_{\max}^3 (1 + e)}$	Extended Hazen equation for sand or gravel

Notes:  $k$  = permeability,  $C_H$  = empirical coefficient,  $d_{10}$  = grain size corresponding to 10% passing,  $C/\mu_o$  = empirical coefficient,  $\mu_o$  = dynamic viscosity of water at 10° C,  $\mu_T$  = dynamic viscosity at temperature  $T$ ,  $n$  = porosity,  $P_{200}$  = percent of material passing the No. 200 sieve,  $C_u$  = coefficient of uniformity,  $e$  = void ratio, and  $e_{\max}$  = maximum void ratio.

Empirical correlation equations for estimating permeability are best suited for materials that are similar to those used to develop the equation. The Hazen (1911) equation was developed for clean filter sands at or near their minimum density ( $\rho_{min}$ ) with uniformity coefficients ( $C_u$ ) of less than 5. The empirical coefficient,  $C_H$ , in this equation is generally considered to vary between 0.8 and 1.5. However, Carrier (2003) has shown that the magnitude of  $C_H$  can vary over several orders of magnitude when applied to different granular materials. Hazen's equation is not expected to perform very well for the aggregates in this study because they contain effective particle sizes ( $d_{10}$ ) larger than the sand that Hazen used to develop his equation, and  $C_u$  values greater than 5.

The Terzaghi (1925) equation takes multiple factors into account including viscosity of the permeant (water) at different temperatures,  $d_{10}$ , and  $n$ . The empirical coefficient in this equation,  $C/\mu_o$ , varies from 460 for angular sands to 800 for rounded sands. A value of 460 was used here due to the crushed nature of the aggregates being examined. This equation was developed for sands with non-uniform grain size and shape. It is more versatile than Hazen's equation because it accounts for more factors that influence permeability. It is unknown if the Terzaghi equation can be successfully applied to soils containing particle sizes larger than sand.

The Moulton (1980) equation was developed for roadway subbase aggregates. It takes multiple factors into account including porosity and the percent passing the No. 200 sieve. This

equation utilizes multiple factors and was developed for materials similar to those used in this study.

The Sahahabi et al. (1984) and Chapuis (2004) equations are both variants of the Kozeny-Carman equation, which is given by:

$$k \left( \frac{\mu}{\gamma_p} \right) = \frac{1}{k_o T^2 S_o^2} \left( \frac{e^3}{1+e} \right) \quad (4)$$

where,  $e$  = void ratio,  $k$  = permeability,  $\mu$  = the dynamic viscosity of the permeant,  $\gamma_p$  = is the unit weight of the permeant,  $k_o$  = the pore shape factor,  $T$  = the tortuosity factor, and  $S_o$  = particle shape factor (Kozeny 1927, Carman 1937).

This equation is widely recognized as a reasonable predictor of permeability in porous media such as gravels, sands, and silts (Carrier 2003). The Kozeny-Carman equation is based on hydraulic principles and takes into account pore shape and size, particle shape and size, and the tortuosity of the flow path. These parameters are difficult to quantify because there is no practical way of measuring the tortuosity of the pore space, and most aggregates contain widely varying pore and particle sizes and shapes, as compared to the single value the equation accounts for.

Many variations of the Kozeny-Carman equation have been developed that utilize different methods of experimentally correlating the pore shape/tortuosity/particle shape term ( $k_o T^2 S_o^2$ ) to more readily measured parameters. The equations presented here from Shahabi et al. (1984) and Chapuis (2004) are both based on the Kozeny-Carman equation. Shahabi et al. (1984) assumed that the  $k_o T^2 S_o^2$  term depends on  $d_{10}$  and  $C_u$ , while Chapuis (2004) assumed that this term depends solely on  $d_{10}$ . The researchers each used different regression techniques and data sets to develop their equations.

Chapuis (2004) also developed what is known as the “extended Hazen” equation, which is essentially another variant of the Kozeny-Carman equation. The extended Hazen equation is nearly the same as the Hazen equation except that it includes a correction factor for the void ratio. Hazen’s equation was developed for loose filter sands. The term “loose” implies that these sands were at or near  $e_{max}$ . The correction factor was developed by Chapuis (2004) to adjust the permeability of a sample that is at an  $e$  other than  $e_{max}$ .

### 3.9.6 Correlation Equations - Results

The empirical correlation equations presented in this study utilize grain size data from mechanical sieve analyses. Two sets of estimated permeabilities are presented; one set utilizes MSU grain size data, and the other set utilizes MDT grain size data. Figure 25 shows a comparative plot of the predicted and measured  $k$  values for the 6A aggregate type utilizing

MSU and MDT grain size data. Differences in  $k$  estimations between the MSU and MDT grain size data are evident in the 6A-Great Falls sample where predicted values of permeability are almost an order of magnitude apart from each other. This exemplifies the dependence of these estimation equations on the finer fraction of the grain size data.

Figure 26 and Figure 27 show comparative plots of the predicted and measured permeabilities for the 5A and 2A aggregate types, respectively. Permeability estimations utilizing MDT gradation data could not be created for the 5A-Kalispell sample because the MDT gradation did not include grain size data with small enough particle sizes to utilize the estimation equations.

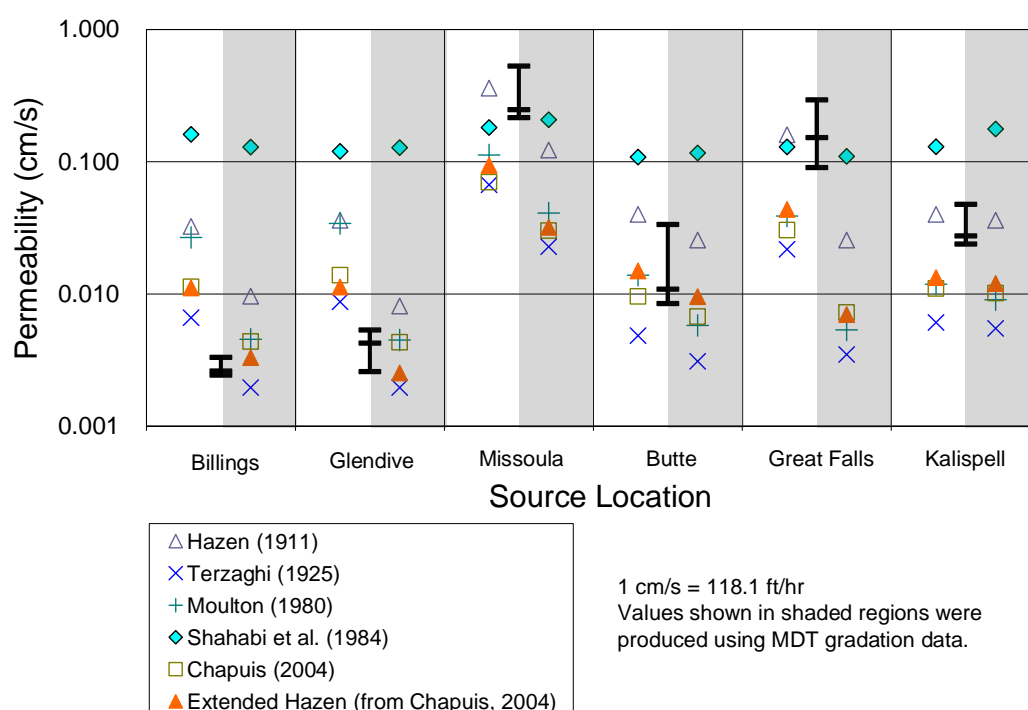


**Figure 25. Calculated permeabilities for the 6A aggregates.**

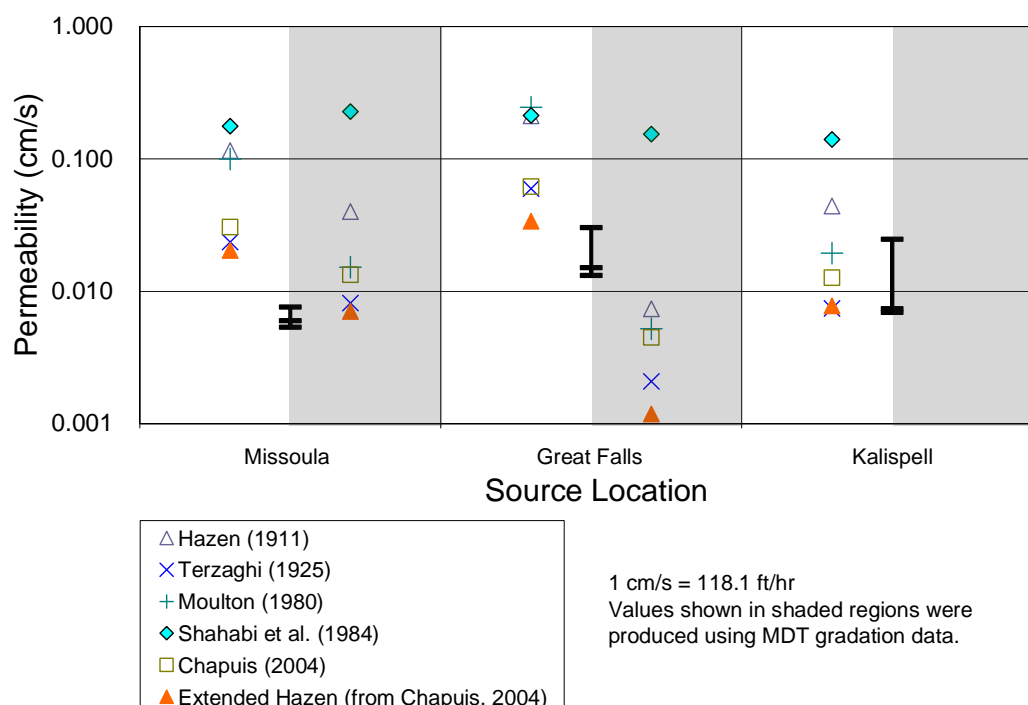


**Figure 26. Calculated permeabilities for the 5A aggregates.**

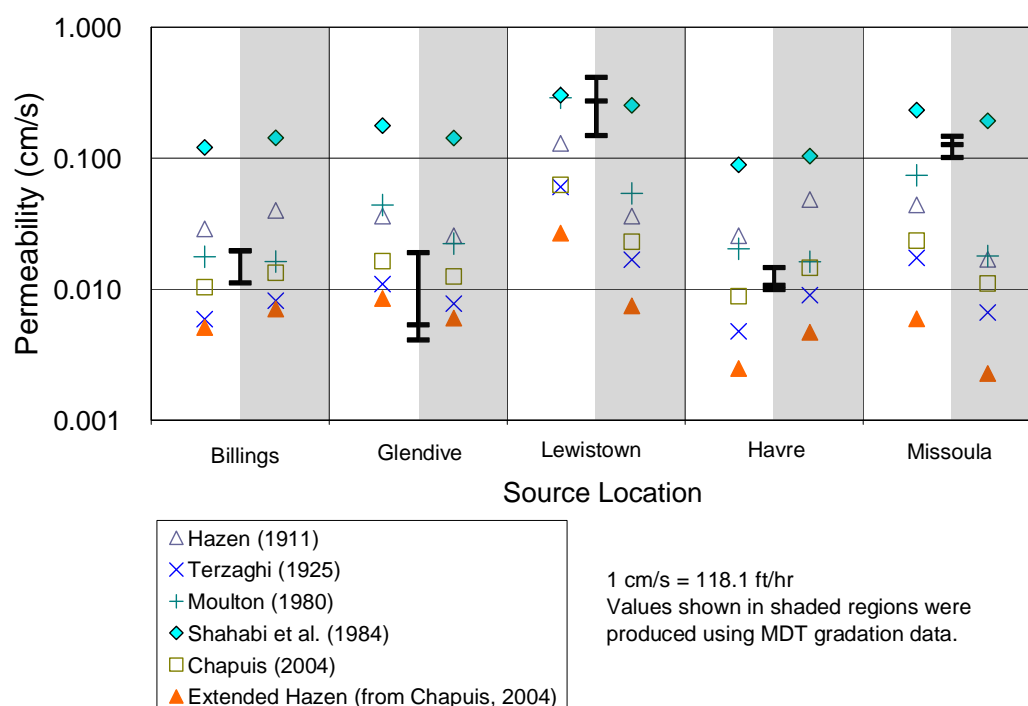


**Figure 27. Calculated permeabilities for the 2A aggregates.**

Ranges of permeability predicted by the correlation equations varied widely, as summarized in Table 13. In many cases, the highest and lowest predicted values of permeability bracketed the measured permeability values. This is true of 6A-Butte, 6A-Kalispell, 5A-Great Falls, 5A-

Kalispell, 2A-Billings, and 2A-Havre. The permeability predictions from the Hazen (1911) and Moulton (1980) equations both tended to fall at or near the upper end of the estimations. While the permeability predictions from the Terzaghi (1925) and extended Hazen (Chapuis, 2004) equations both fell at or near the lower end of the estimations. The equations from Chapuis (2004) and Moulton (1980) tended to fall somewhere in between these high and low values.

The equation developed by Shahabi et al. (1984) generally over predicted permeability for the aggregates in this study. This equation was not very sensitive to its inputs because predicted values of  $k$  did not change significantly even when there were notable changes in grain size distribution.

The estimated permeabilities generally rise and fall in a similar manner to the measured values for each aggregate type as shown in Table 13, Figure 25, Figure 26, and Figure 27. These trends coupled with the bracketing effect of the predicted permeability values by the measured values indicates that the measured permeabilities are reasonable based on past studies by others.

**Table 13. Ranges of Predicted Permeability Based on Aggregate Type**

<b>Prediction Equation</b>	<b>CBC-6A (cm/s)</b>	<b>CBC-5A (cm/s)</b>	<b>CTS-2A (cm/s)</b>
Hazen (1911)	0.021-0.002	0.078-0.044	0.083-0.031
Terzaghi (1925)	0.015-0.004	0.016-0.007	0.039-0.007
Moulton (1980)	0.077-0.010	0.057-0.020	0.172-0.017
Shahabi et al. (1984)	0.195-0.113	0.203-0.140	0.278-0.097
Chapuis (2004)	0.045-0.008	0.022-0.013	0.043-0.012
Extended Hazen (Chapuis, 2004)	0.063-0.007	0.014-0.008	0.017-0.004
Measured Values	0.186-0.002	0.030-0.005	0.273-0.004

Note: The predicted permeability ranges are based on averages from both the MSU and MDT data.

### 3.9.7 Void Ratio-Permeability Relationships

In addition to particle size and particle size distribution,  $k$  is affected by pore size, pore shape, and tortuosity. These pore characteristics are in turn affected by the state of compaction. For cohesionless soils, the state of compaction is often quantified on a macro basis by void ratio ( $e$ ). The permeameter samples in this study were each compacted using the same compaction energy and methodology; however, because of differences in particle size, shape, and distribution, the compacted void ratios varied slightly between samples. Because of the dependency of  $k$  on void structure, a relationship between  $e$  and  $k$  was explored. When all soil samples are examined together, there is not a very strong correlation between  $e$  and  $k$ , as shown

in Figure 28. This indicates that  $k$  cannot be predicted solely on the basis of compacted density or  $e$ .

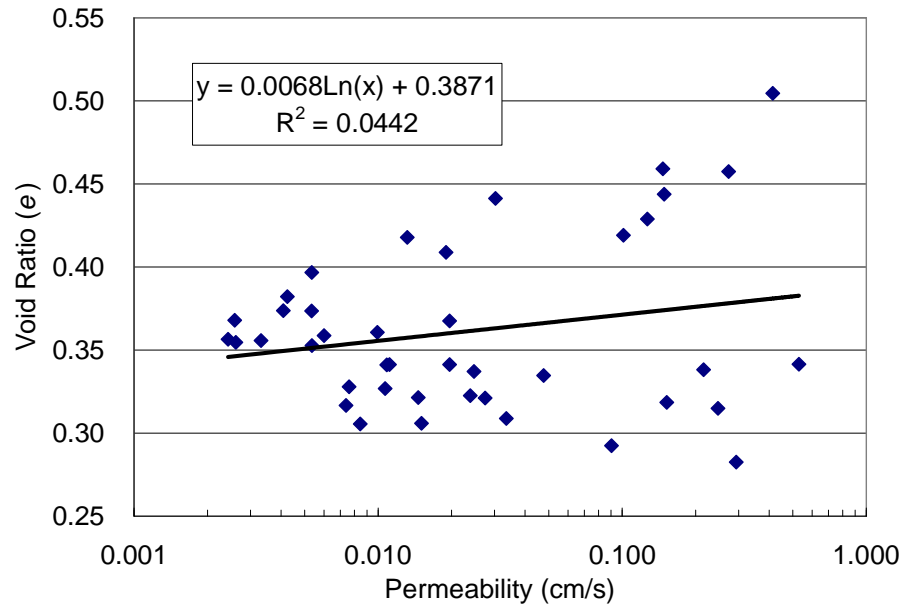


**Figure 28. Void ratio versus permeability for all aggregates in this study.**

The value of  $e$  commonly used to calculate  $k$  is the average  $e$  determined from weight-volume relationships using total weight and total volume data. Cote and Konrad (2003) proposed that because  $k$  is known to highly depend on smaller particles, it could be better correlated by considering only the finer fraction of a base course aggregate. The average  $e$  is a function of both fine fraction and coarse fraction void ratios. By isolating only the fine fraction void ratio ( $e_f$ ), a more accurate prediction of  $k$  may be possible. The cutoff size between fine and coarse fractions depends on the material size and particle distribution – the cutoff is not necessarily the No. 200 sieve size.

The following equation for calculating  $e_f$  has been modified from Cote and Konrad (2003):

$$e_f = \frac{e}{F} = \frac{G_s \gamma_w - \gamma_d}{F \gamma_d} \quad (5)$$

where,  $e$  = void ratio,  $e_f$  = void ratio of the finer fraction,  $F$  is the percent fines based on the No. 10 sieve,  $\gamma_d$  = dry unit weight,  $G_s$  = specific gravity, and  $\gamma_w$  = unit weight of water.

Based on a parametric study of sieve sizes, the No. 10 sieve was selected as the cut-off size between fine and coarse for determining the percent of fine material for use in Equation (5). A comparison of  $e_f$  versus  $k$  is shown in Figure 29. The utilization of  $e_f$  provides a significantly better correlation than  $e$ , although there is still some scatter in the data.

Equation (5) requires the assumption that fine particles are evenly distributed in the void space of the coarse particle skeleton. This assumption is valid for aggregates with enough fine particles to fill the coarse particle void space. The validity of this assumption is called into question for aggregates that have insufficient fine particles to completely fill the coarse fraction void space. This is difficult to quantify and likely accounts for some of the remaining scatter in the data.

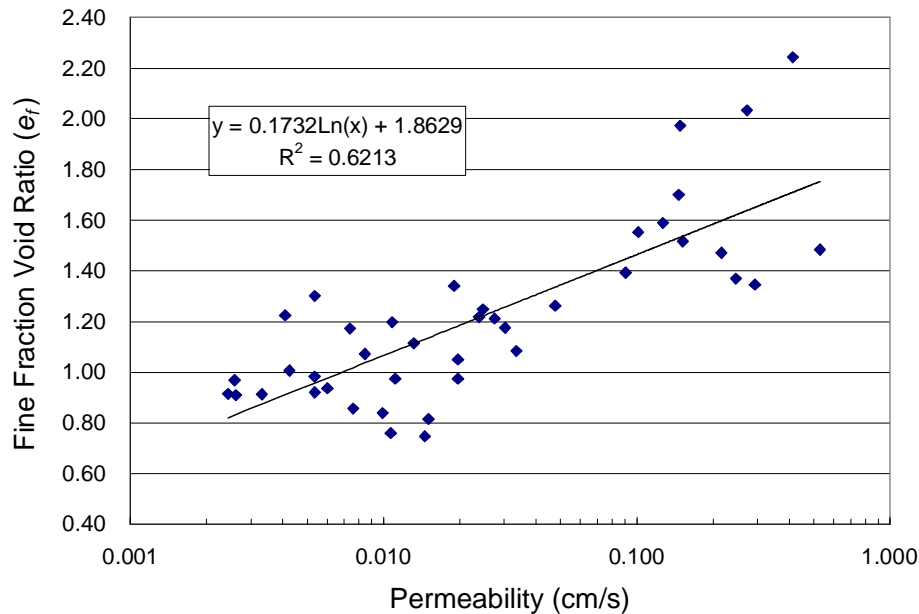


**Figure 29. Fine fraction void ratio ( $e_f$ ) versus permeability.**

Several other correlations were examined using  $C_u$ ,  $C_s$ , and  $d_{10}$ ; however, none of these other parameters were effective at reducing  $R^2$ . This suggests that hydraulic properties of an aggregate rely more heavily on pore parameters than particle parameters. According to Equation (5),  $e_f$  is a function of  $e$  and  $F$ , which is derived from the grain size distribution (percent fines based on the No. 10 sieve). Aggregate compaction is often specified as some percentage of a maximum laboratory determined density, or unit weight. Based on the data evaluation and logarithmic regression shown in Figure 29, the following equation is presented for estimating permeability for base course materials used by MDT:

$$\ln k = \frac{1}{0.17F} \left[ \frac{G_s \gamma_w}{RC \gamma_{d \max}} - 1 \right] - 10.77 \quad (6)$$

where,  $k$  is the permeability in cm/s,  $F$  is the percent material finer than the No. 10 sieve,  $G_s$  is the specific gravity,  $\gamma_w$  is the unit weight of water in pcf,  $\gamma_{d \max}$  is the maximum unit weight in pcf, and  $RC$  is the relative compaction.



This equation could be useful for comparing the hydraulic properties of base course aggregates, for estimating the hydraulic properties of materials that are out of specification, or to determine the maximum amount of material passing the No. 10 sieve to achieve a particular minimum  $k$ .

Equation (6) can be re-arranged to compute  $F$  (the maximum amount of material passing the No. 10 sieve) if  $G_s$ ,  $\gamma_{d \max}$ , the required  $RC$ , and the required minimum  $k$  are all known. This is a useful application of the equation for developing material specifications, and is presented as:

$$F = \left[ \frac{1}{0.17 \ln k + 1.83} \right] \left[ \frac{G_s \gamma_w}{RC \gamma_{d \max}} - 1 \right] \quad (7)$$

The following steps outline the calculation procedure:

1. Determine  $\gamma_{d \max}$  from either maximum index density or modified Proctor testing.
2. Assume a value for  $RC$ . MDT commonly uses 0.95 to 0.98.
3. Measure  $G_s$  in the lab, or assume a value of about 2.7.
4. Select a minimum value of  $k$ . This value should be selected so that it is practically achievable, and will provide adequate drainage capacity. Table 14 shows AASHTO (1993) design guide recommended minimum permeabilities.
5. Substitute the above parameters into Equation (7) to determine the maximum amount of material passing the No. 10 sieve.

**Table 14. 1993 AASHTO Minimum Permeability Recommendations**

Quality of Drainage	Minimum Permeability		Time to Drain
	ft/hr	cm/s	
Excellent	41.67	0.353	2 hours
Good	3.54	0.030	1 day
Fair	0.46	0.004	1 week
Poor	0.02	0.0002	1 month
Very poor	0.0008	0.00007	Water will not drain

Following is an example calculation.

1.  $\gamma_{d\max}$  is determined from maximum index density testing to be 138 pcf.
2. The required degree of  $RC$  is assumed to be 0.98, as is commonly used by MDT for the base course.
3.  $G_s$  is determined from laboratory testing to be 2.70.
4. A minimum value of  $k$  is assumed to be 0.01 cm/s because it is practical and achievable for these materials based on Figure 29, and will provide fair to good drainage based on the minimum values provided in Table 14.
5. The values are substituted into Equation (7) and  $F$  is calculated.

$$F = \left[ \frac{1}{0.17 \ln(0.01) + 1.83} \right] \left[ \frac{(2.70)(62.4)}{(0.98)(138)} - 1 \right] = \left[ \frac{1}{1.047} \right] \left[ \frac{168.48}{135.24} - 1 \right] = 0.235$$

**Solution:** For this material, there can be a maximum of 23.5% of material passing the No. 10 sieve to ensure the desired minimum  $k$  is achieved.

## 4 SUMMARY & CONCLUSIONS

This report details a laboratory analysis of three different grades of MDT aggregates. Two of these grades were crushed base course materials (CBC-6A and CBC-5A) and the other grade was a crushed top surfacing material (CTS-2A). CTS materials have smaller maximum particle sizes than CBC materials because they are intended for different uses. CBC materials are used as full depth base course aggregate layers, while CTS materials are typically used in relatively thin lifts over the CBC aggregate layer to provide a smooth flat surface for the placement of asphalt concrete.

The primary goal of this laboratory analysis was to quantify differences in engineering properties of these three material types. This information could be used to alleviate confusion among designers and District personnel regarding differences in customary practices, and to provide valuable information to construction personnel when faced with requests by contractors to change or substitute aggregate types.

The engineering properties examined in this study were: compaction, durability, strength, stiffness, and drainage. These properties were quantified by synthesizing and analyzing results from the following laboratory tests:

- Ø geotechnical index tests,
- Ø direct shear,
- Ø R-value,
- Ø permeability, and
- Ø Los Angeles abrasion/degradation.

Statistical analyses of average values based on material type were conducted using the two sample t-test to determine if apparent trends in measured laboratory test results represented true differences between aggregate types.

Direct shear tests were performed to quantify the strength and stiffness of the materials. Several parameters were quantified during this testing including the initial stiffness ( $k_i$ ), the secant stiffness ( $k_u$ ), and the effective friction angle ( $\phi'$ ). Another test that is used to quantify the strength and stiffness of a material is the R-value test. The R-value test is used by MDT to evaluate the stiffness, strength, and stability of subgrade and base materials. All R-value tests were completed by MDT at their Helena materials testing lab. Trends in comparing average values of these various strength/stiffness parameters based on material type are summarized in Table 15.

In summary, the CBC-6A aggregates generally exhibited the highest strength and stiffness of the three material types. The CBC-6A aggregates exhibited higher  $k_i$  and  $k_u$  values than both the CBC-5A and CTS-2A material types. On average, the CBC-6A aggregates exhibited higher  $\phi'$  values and higher R-values than the CTS-2A materials. In terms of strength parameters

measured from direct shear tests, there was no statistically significant difference between CBC-5A and CTS-2A materials. The CBC-6A and 5A materials exhibited similar average R-values, which were both slightly greater than the CTS-2A materials. Overall, the CTS-2A materials generally exhibited the lowest average strength and stiffness. Although this material was the poorest performer when compared to the two CBC materials, it still exhibited relatively high strength and stiffness.

**Table 15. Summary of Key Test Results**

$k_i$	$k_u$	$\phi'$	R-value	Permeability
6A > 5A	6A > 5A	6A = 5A	6A = 5A	6A > 5A
6A > 2A	6A > 2A	6A > 2A	6A > 2A	6A = 2A
5A = 2A	5A = 2A	5A = 2A	5A > 2A	5A < 2A

Drainage capacity was quantified using saturated constant head permeability tests. There was some scatter in the measured permeability ( $k$ ) results; however, trends based on material type averages could still be statistically discerned, as summarized in the last column of Table 15. The CBC-6A and CTS-2A materials exhibited the highest average  $k$  values, while the CBC-5A materials exhibited the lowest. Permeability was shown to depend more on the fine fraction void ratio ( $e_f$ ) than on aggregate type or maximum particle size. A method of predicting  $k$  based on  $e_f$  was developed, which will allow MDT designers to estimate  $k$  based on gradation and state of compaction. This equation could be useful for comparing the hydraulic properties of base course aggregates, for estimating the hydraulic properties of materials that are out of specification, or to determine the maximum amount of material passing the No. 10 sieve to achieve a particular minimum  $k$ .

LA abrasion testing was performed to quantify the durability of the aggregates. CBC-5A-Missoula and CTS-2A-Havre did not meet MDT durability specifications based on LA Abrasion testing. Results from the LA abrasion tests did not show any trends with regard to material type. It is hypothesized that the durability measurement in this test depends heavily on the mineralogy of the aggregate.

Based on the results from strength, stiffness, and drainage testing, the CBC-6A materials were generally the best performers in this study. The CBC-5A aggregates generally exhibited the second highest strength and stiffness, but also had the lowest drainage capacity. The CTS-2A aggregates generally exhibited the lowest strength and stiffness, but had relatively good drainage capacity. The ability to substitute CTS-2A material for CBC aggregates depends on the relative importance that is assigned to strength, stiffness, and drainage in the pavement design model.

---

## 5 REFERENCES

- AASHTO (1993). American Association of State Highway Transportation Officials. "AASHTO Guide for Design of Pavement Structures." Washington, D.C.
- Bowles, J.E. (1992). "Engineering Properties of Soils and their Measurement." 4th Ed., McGraw-Hill, NY, 241 p.
- Carman, P.C. (1937). "Fluid Flow Through a Granular Bed." *Transactions of the Institution of Chemical Engineers*, Vol. 15, 150 p., London, England.
- Carrier, W.D. (2003). "Goodbye, Hazen; Hello, Kozeny-Carman." *Journal of Geotechnical and Geoenvironmental Engineering*, 129 (11): 1054-1056.
- Chapuis, R. P. (2004). "Predicting the Saturated Hydraulic Conductivity of Sand and Gravel using Effective Diameter and Void Ratio." *Canadian Geotechnical Journal*, 41 (5): 787-795.
- Cote, J. and Konrad, J.M. (2003). "Assessment of the Hydraulic Characteristics of Unsaturated Base-Course Materials: A Practical Method for Pavement Engineers." *Canadian Geotechnical Journal*, 40 (1): 121-136.
- Das, B.M. (2002). "Principles of Geotechnical Engineering." 5<sup>th</sup> Ed., Brooks/Cole, CA, 589 p.
- Hazen, A. (1911). Discussion of "Dams on Sand Foundations." by A.C. Koeing, *Transactions*, ASCE (American Society of Civil Engineers), Vol. 73: 199-203.
- Holtz, R.D. and Kovacs, W.D. "An Introduction to Geotechnical Engineering." Prentice Hall, Englewood Cliffs, New Jersey, 733 p.
- Kozeny, J. (1927). "Über kapillare Leitung des Wassers in Boden," *Sitzungsberichte der Wiener Akademie der Wissenschaften*, Vol. 136, Part 2A: 271-306 (in German).
- Moulton, L.K. (1980). "Highway Subdrainage Design." Report No. FHWA-TS-80-224, Federal Highway Administration.
- PCA (Portland Cement Association). (1966). "Thickness Design for Concrete Pavements."
- Shahabi, A.A., Das, B.M., and Tarquin, A.J. (1984). "An Empirical Relation for Coefficient of Permeability of Sand." Proceedings of the Fourth Australia-New Zealand Conference on Geomechanics, Vol. 1: 54-57.
- Terzaghi, C. (1925). "Principles of Soil Mechanics: III-Determination of Permeability of Clay." *Engineering News Record*, 95 (21): 832-836.
- Thornton, S.I. and Toh, C.L. (1995). "Permeability of Pavement Base Course." Report No. MBTC FR 1010, Arkansas Highway and Transportation Department, Little Rock, AR,

and Mack-Blackwell National Rural Transportation Study Center, University of Arkansas, Fayetteville.

Van Til, C.J., McCullough, B.F., Vallerger, B.A., and Hicks, R.G. (1972). "Evaluation of AASHO Interim guides for Design of Pavement Structures." Report No. NCHRP 128, Highway Research Board.

## **APPENDIX A. MDT GRAIN SIZE DISTRIBUTION ANALYSIS PLOTS**

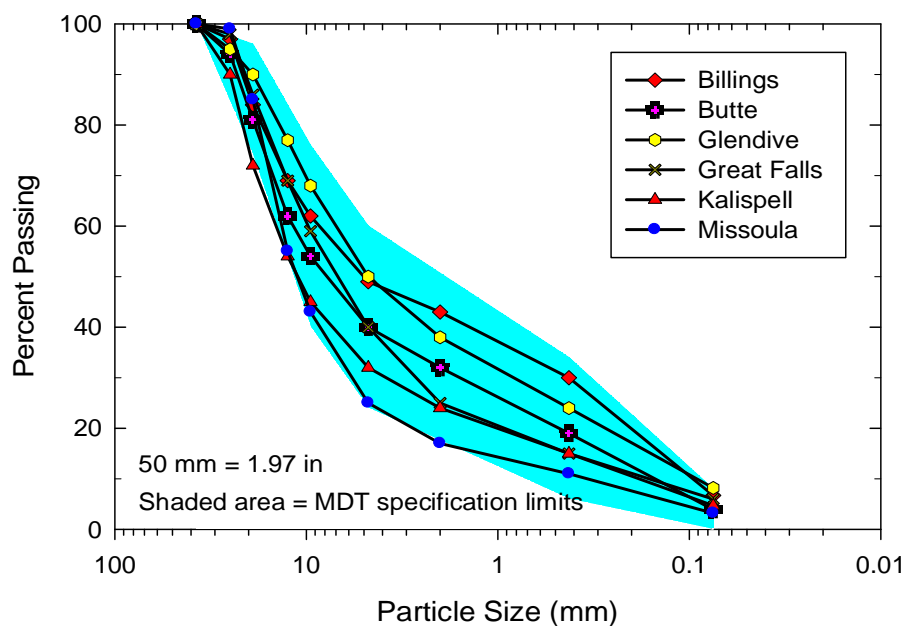


**Figure A 1. CBC-6A gradation results from MDT soils lab.**

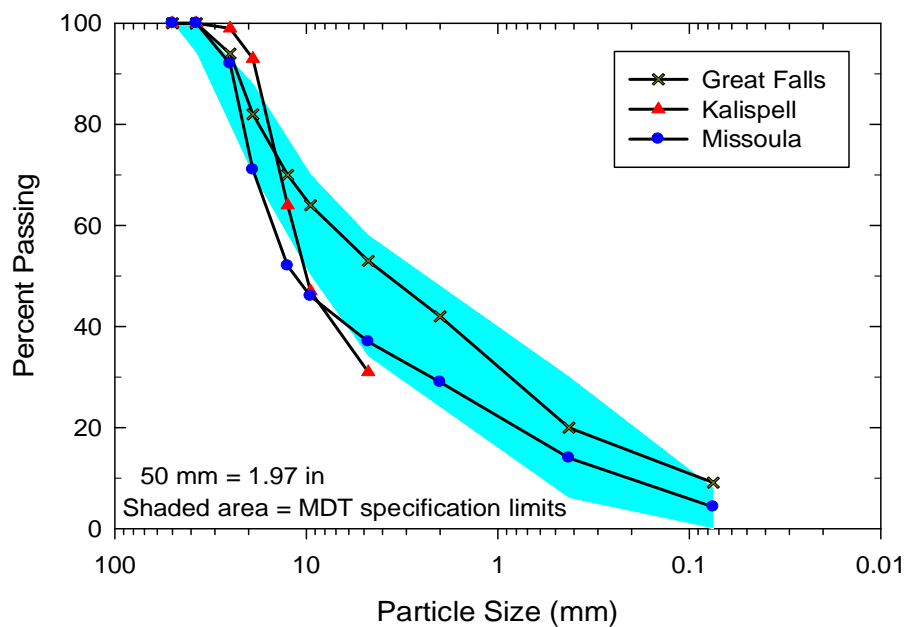


**Figure A 2. CBC-5A gradation results from MDT soils lab.**



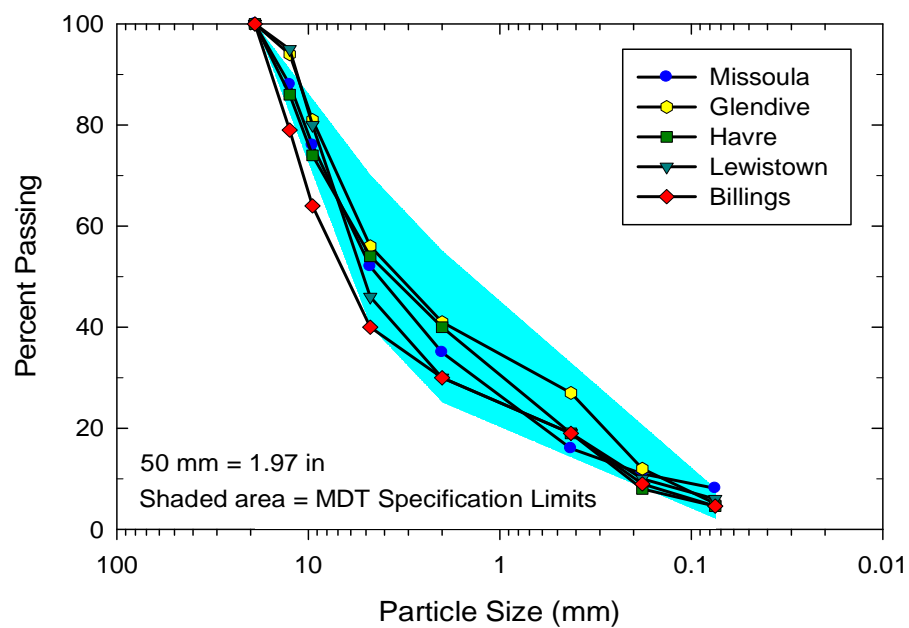


**Figure A 3. CBC-5A gradation results from MDT soils lab.**

## **APPENDIX B. R-VALUE TEST REPORTS**

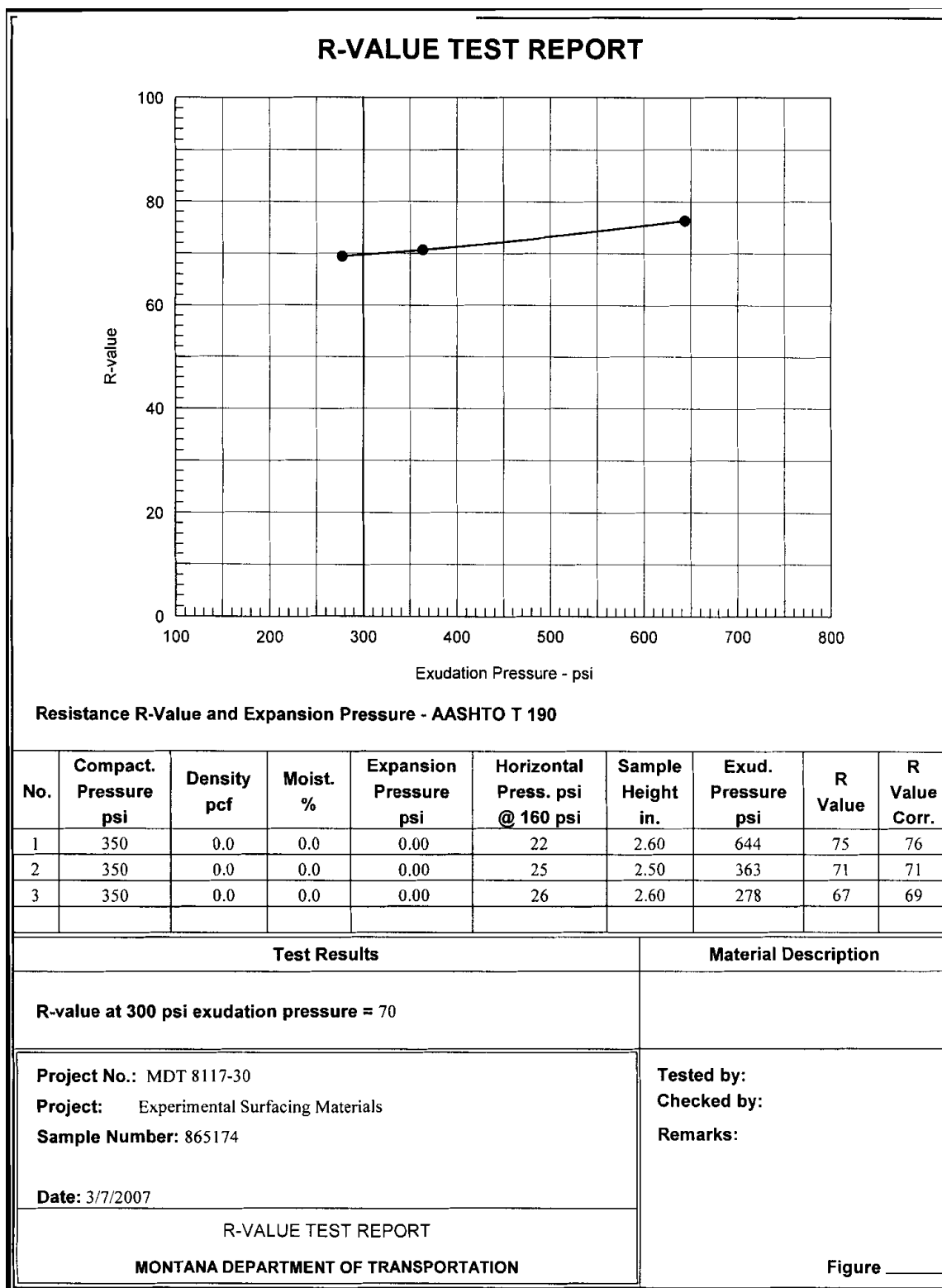


Figure B 1. R-value test report for 2A-Havre.

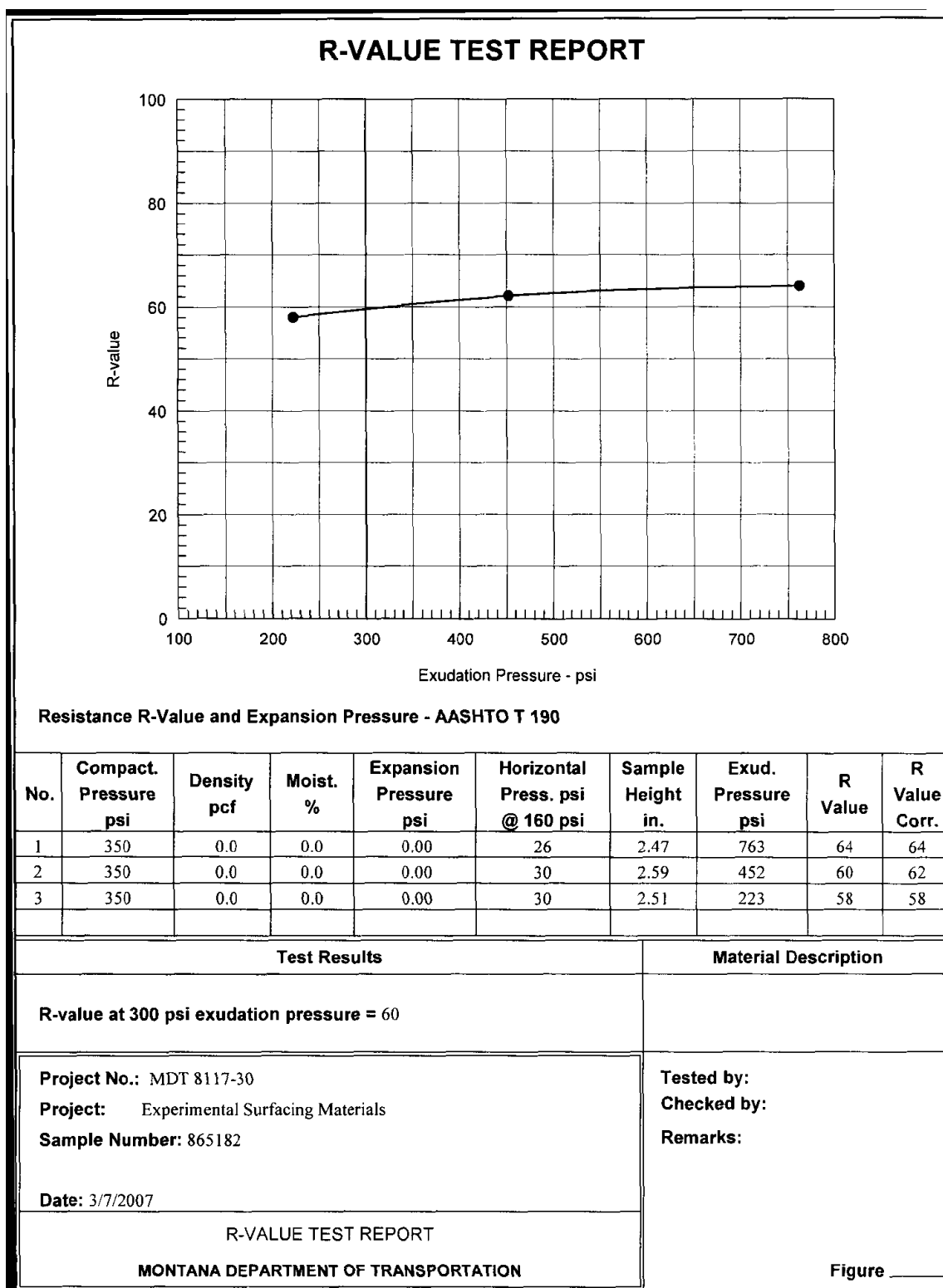


Figure B 2. R-value test report for 2A-Glendive.

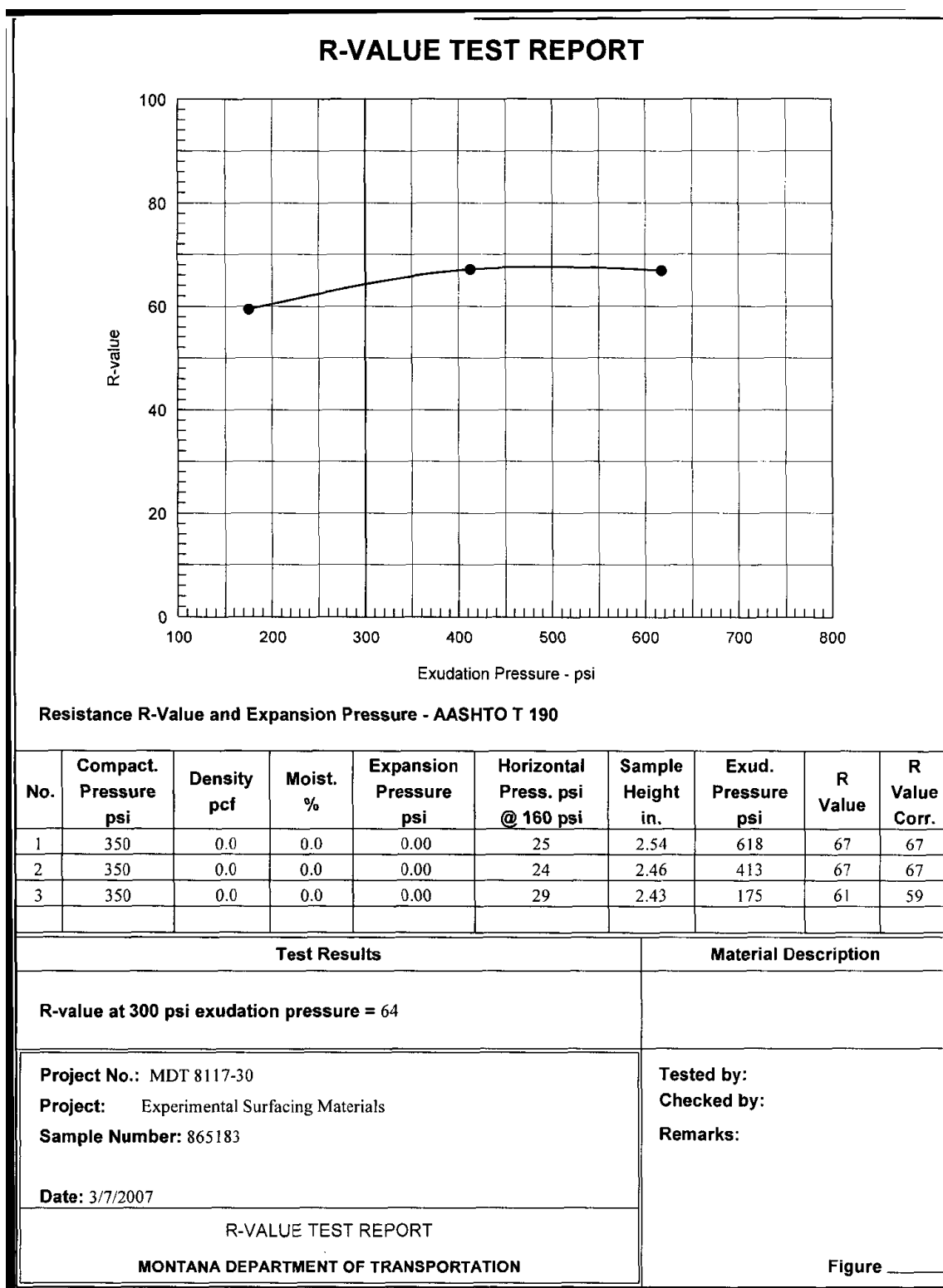


Figure B 3. R-value test report for 2A-Missoula.

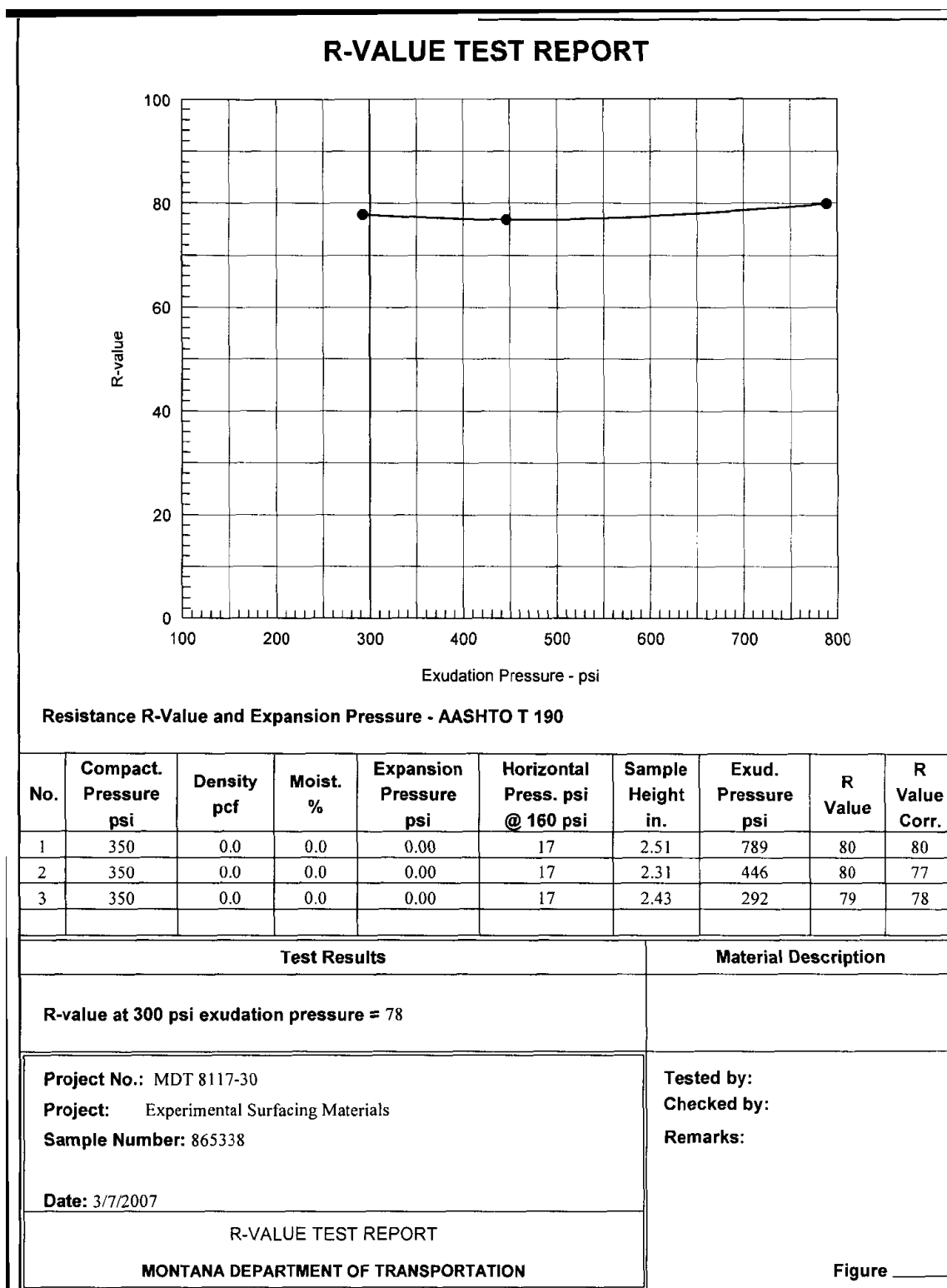


Figure B 4. R-value test report for 2A-Lewistown.

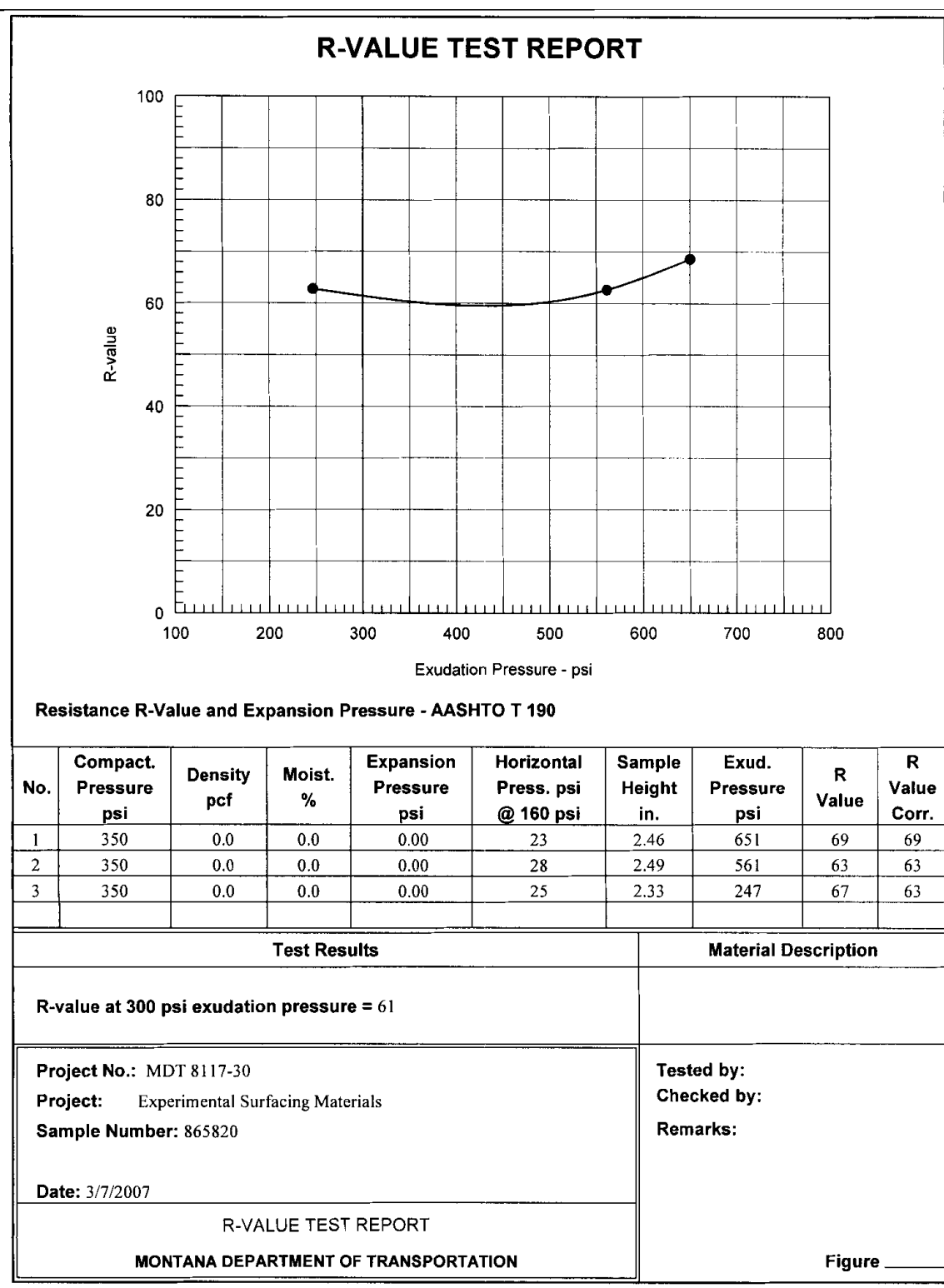


Figure B 5. R-value test report for 2A-Billings.

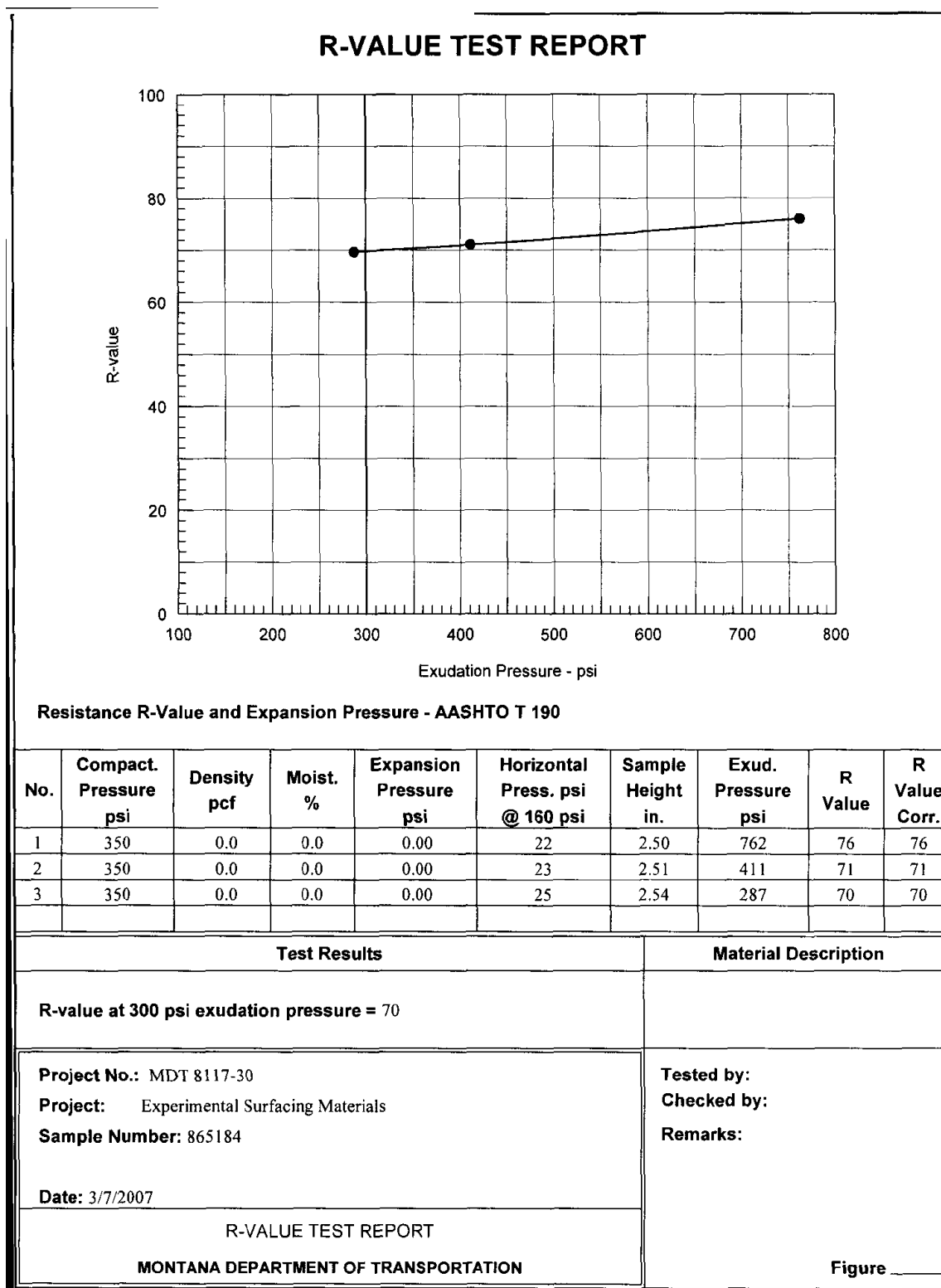


Figure B 6. R-value test report for 5A-Missoula.



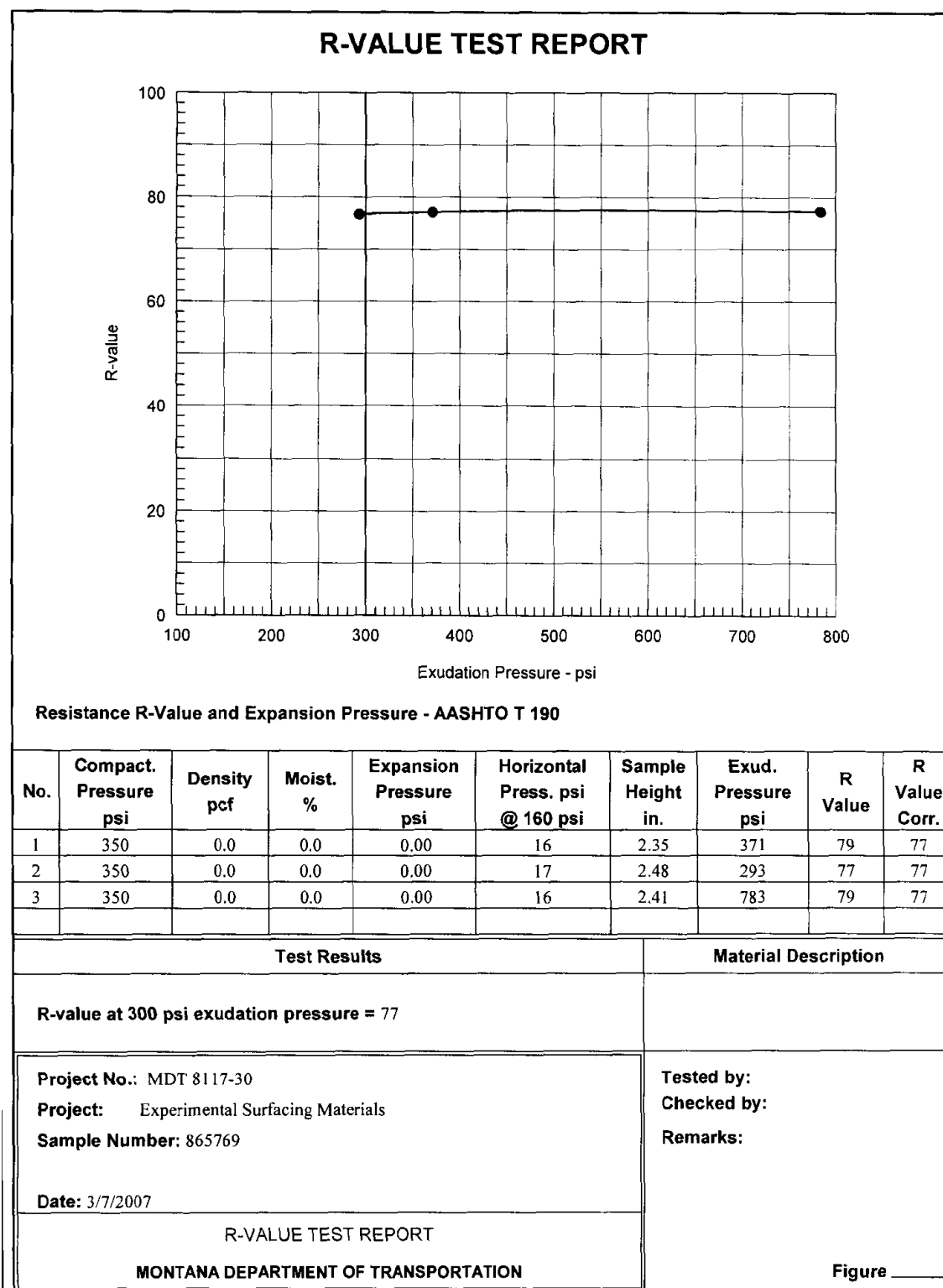


Figure B 7. R-value test report for 5A-Kalispell.

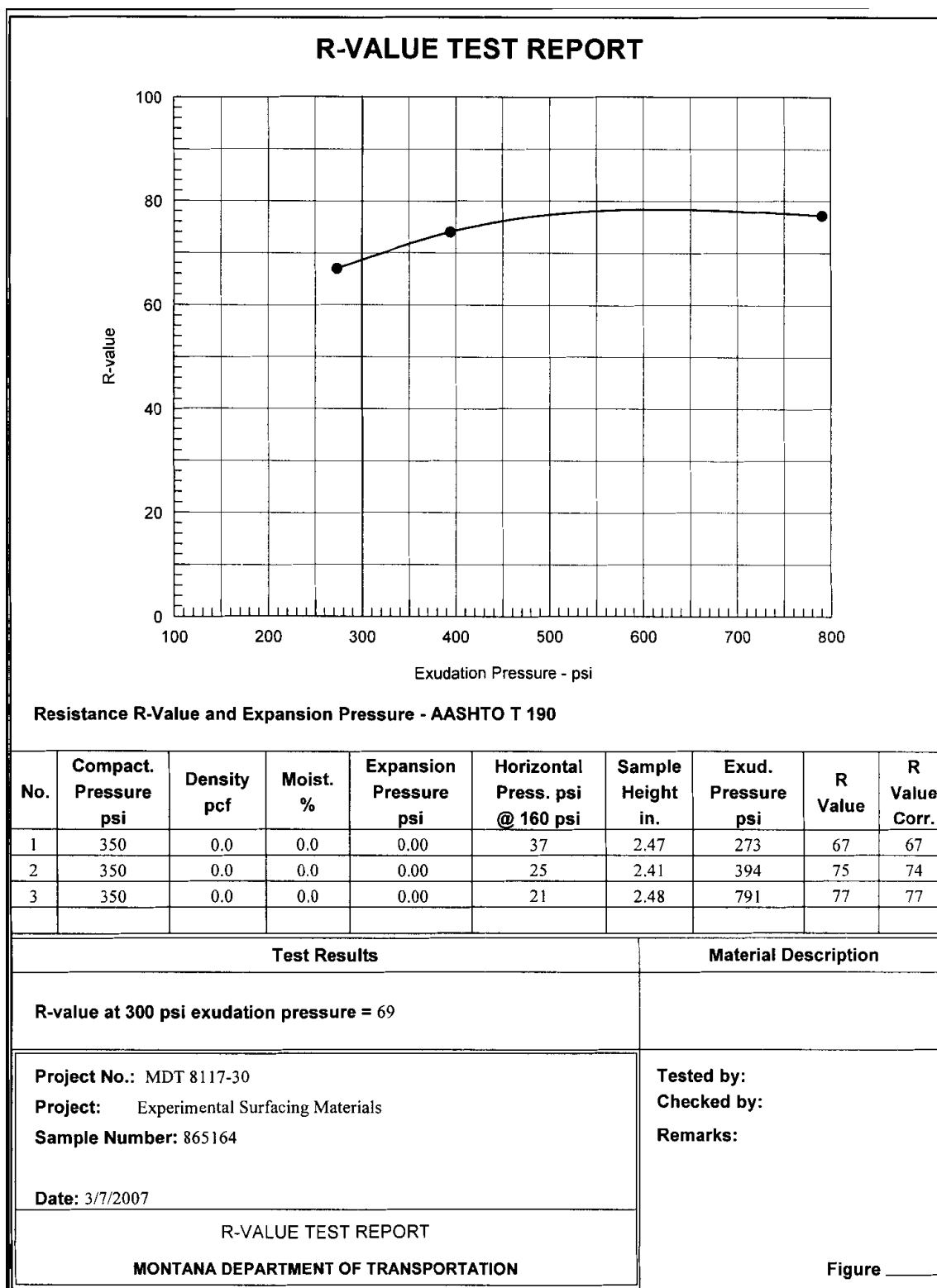


Figure B 8. R-value test report for 5A-Great Falls.

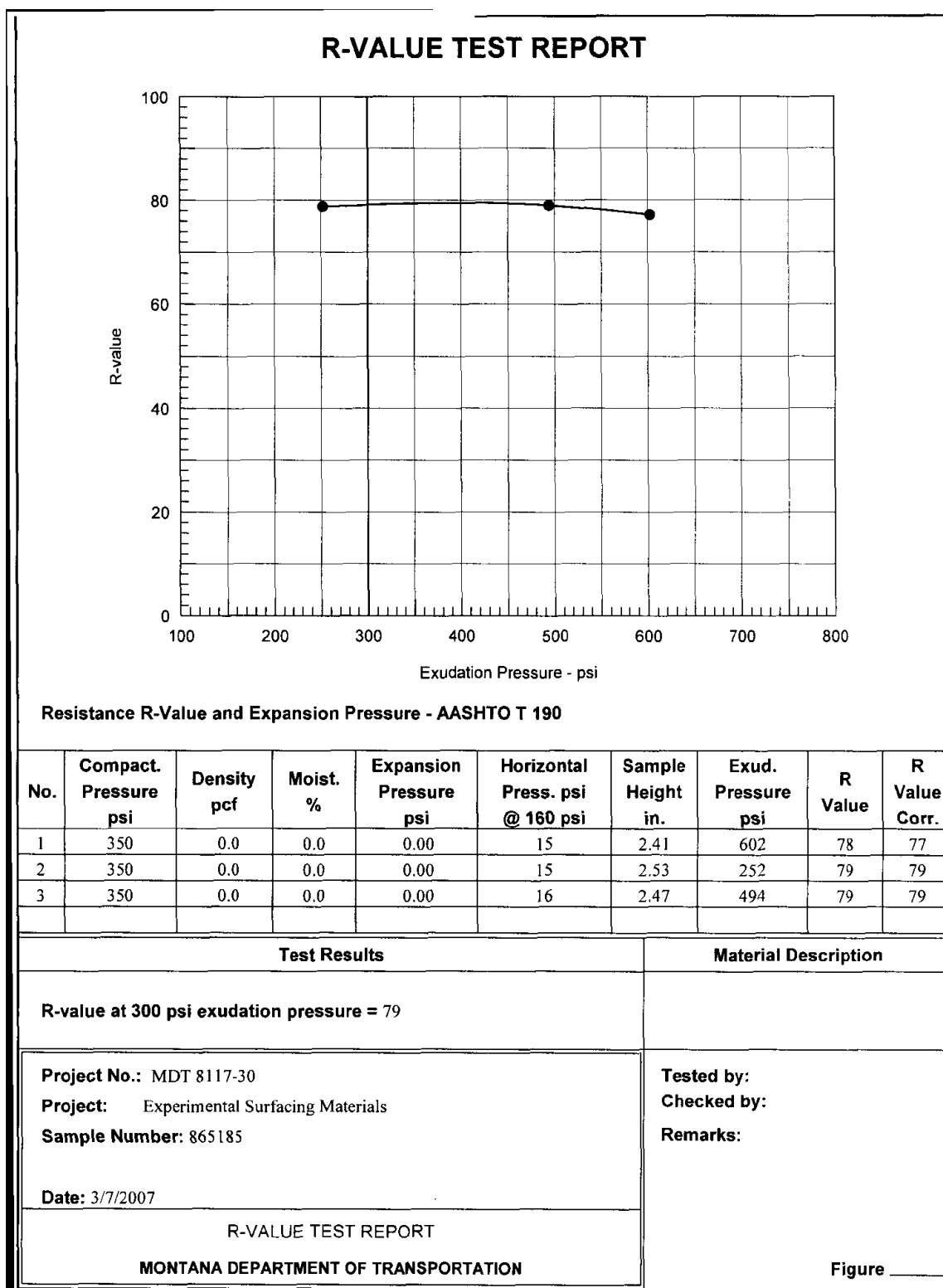


Figure B 9. R-value test report for 6A-Missoula.

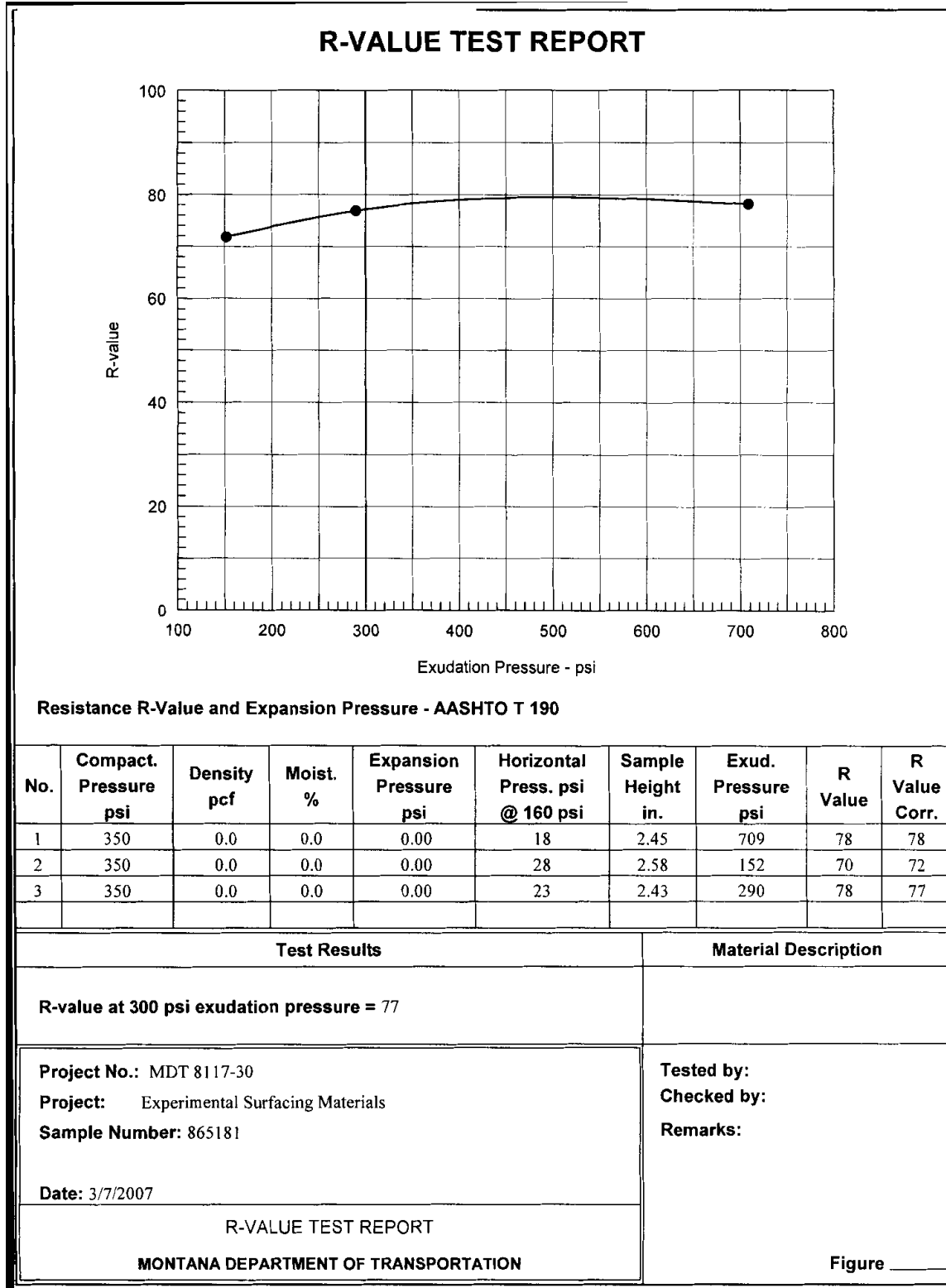


Figure B 10. R-value test report for 6A-Glendive.

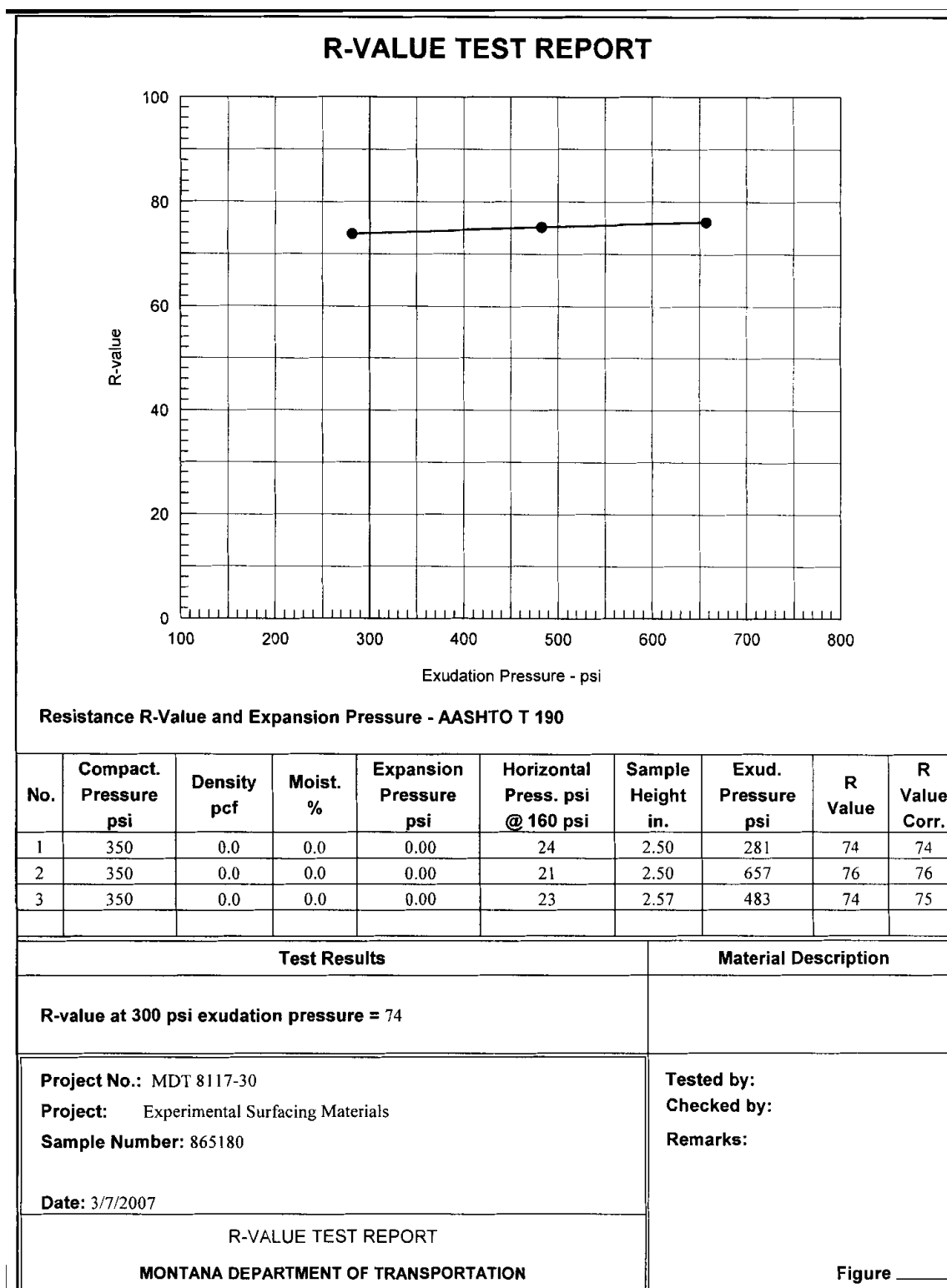


Figure B 11. R-value test report for 6A-Billings.

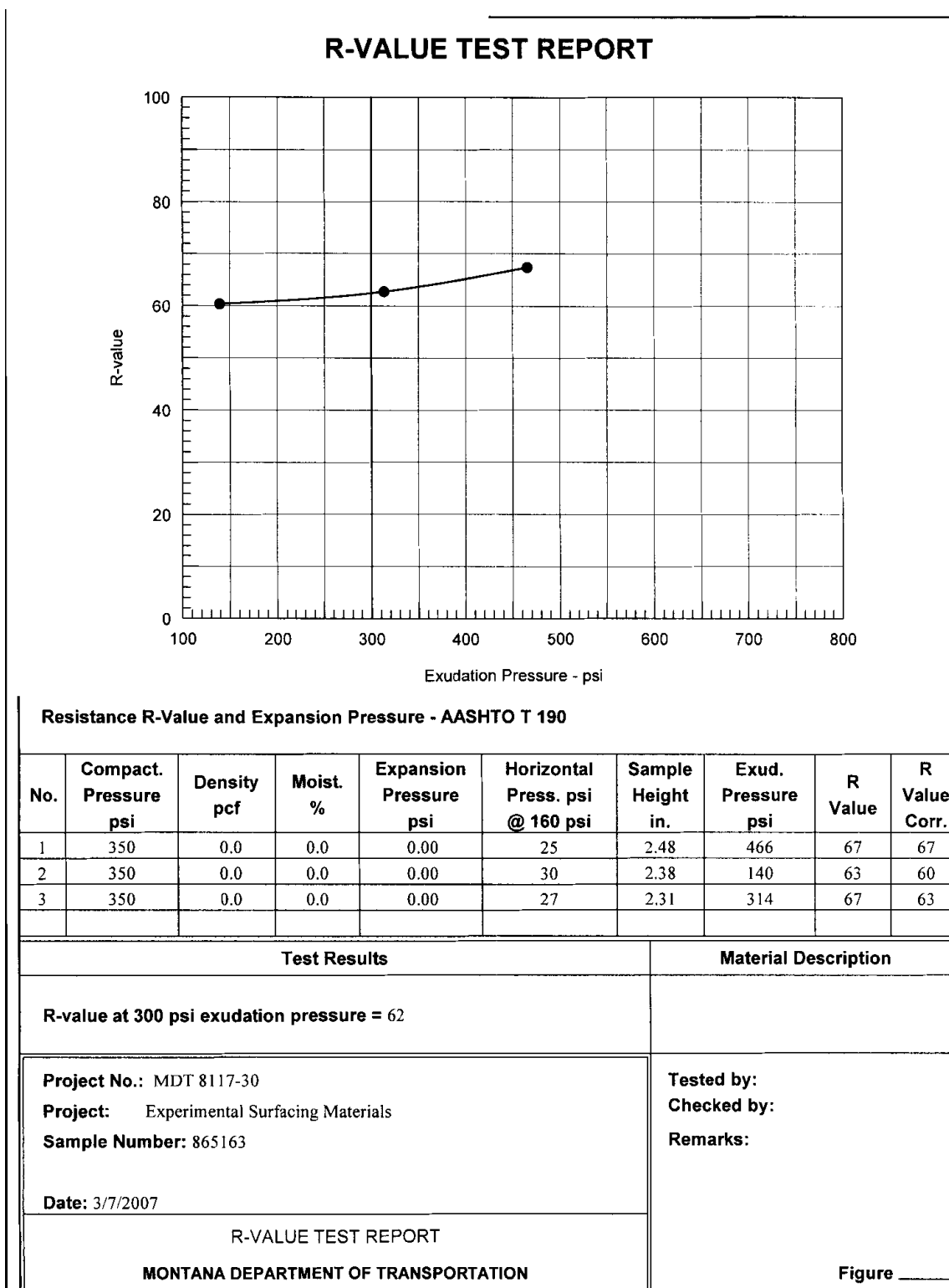


Figure B 12. R-value test report for 6A-Great Falls.

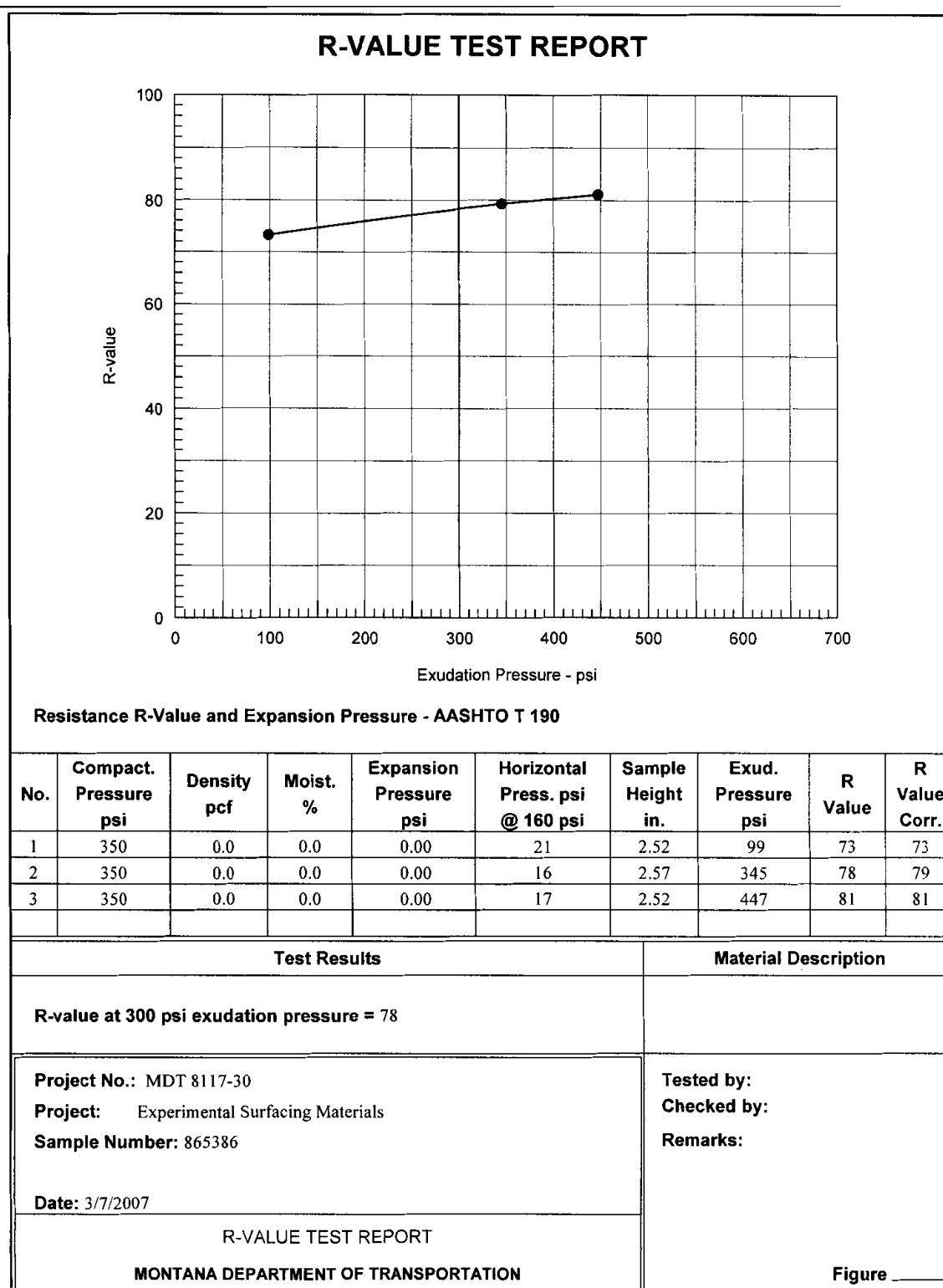


Figure B 13. R-value test report for 6A-Butte.

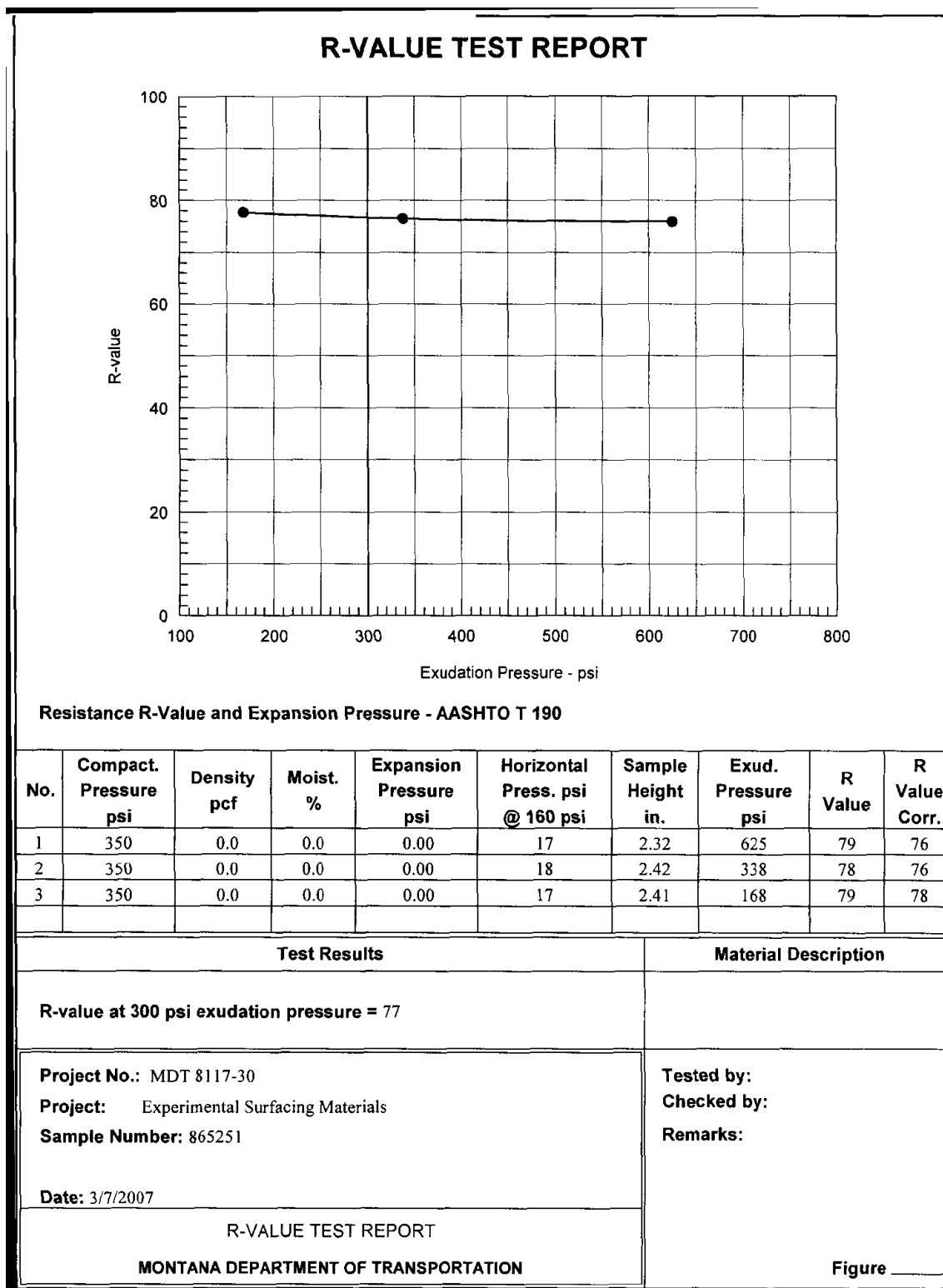
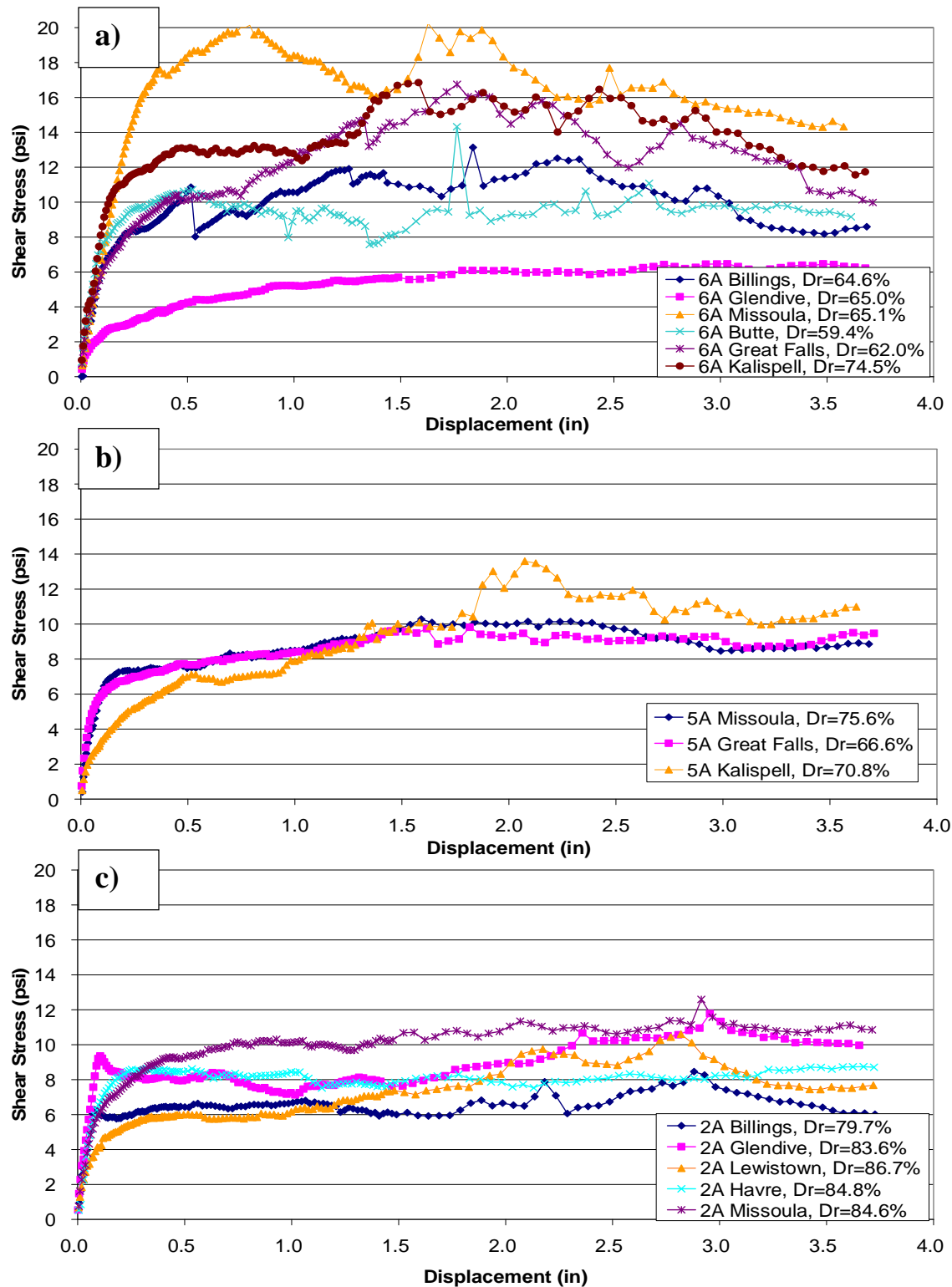


Figure B 14. R-value test report for 6A-Kalispell.



## **APPENDIX C. SHEAR STRESS-DISPLACEMENT PLOTS**



**Figure C 1. Shear stress-displacement plots for 5 psi normal stress: a) 6A samples, b) 5A samples, and c) 2A samples.**

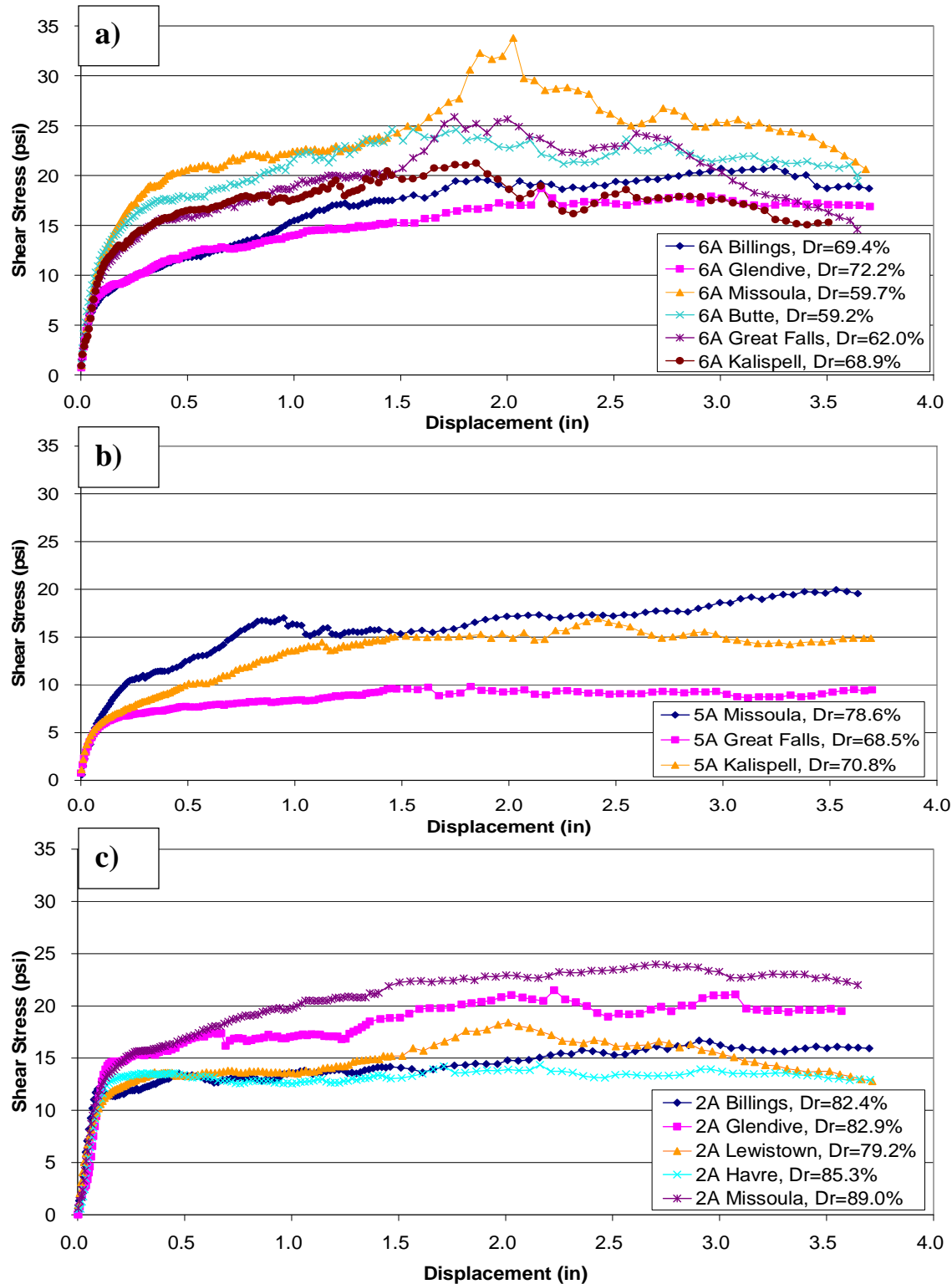


**Figure C 2. Shear stress-displacement plots for 10 psi normal stress: a) 6A samples, b) 5A samples, and c) 2A samples.**

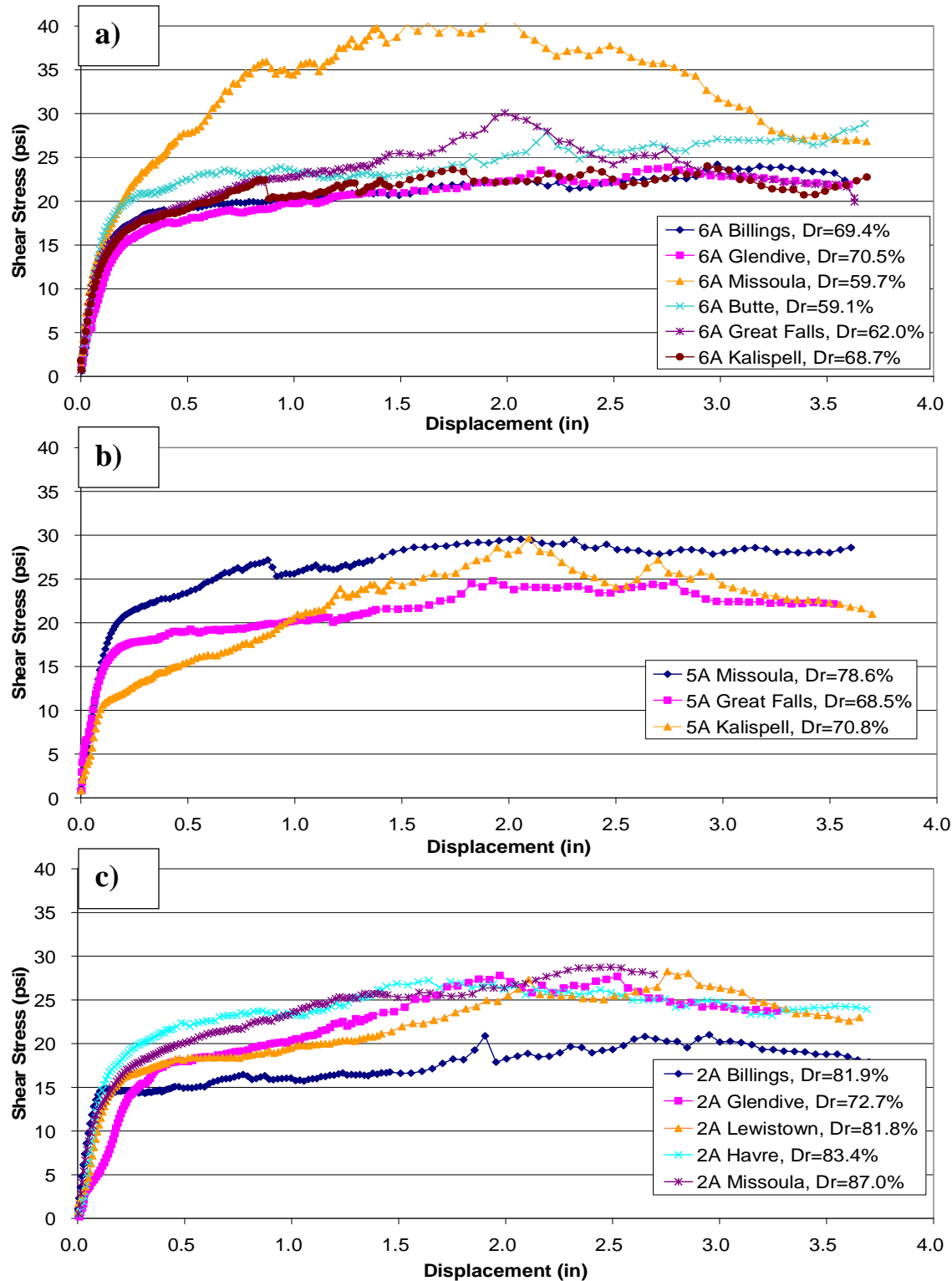


**Figure C 3. Shear stress-displacement plots for 15 psi normal stress: a) 6A samples, b) 5A samples, and c) 2A samples.**

130 copies of this public document were produced at an estimated cost of \$2.39 each, for a total cost of \$310.34. This includes \$168.27 for postage and \$142.07 for printing.